

Accounts

Catalysis on Electron Transfer and the Mechanistic Insight into Redox Reactions

Shunichi Fukuzumi

Department of Applied Chemistry, Faculty of Engineering, Osaka University, Suita, Osaka 565

(Received August 27, 1996)

Both thermal and photoinduced electron transfer reactions from one-electron reductants to various organic oxidants such as carbonyl compounds are catalyzed by the presence of acids and metal ions. The acceleration of rates of electron transfer is ascribed to the thermodynamic stabilization of products of electron transfer by the protonation or complexation with metal ions, which results in the positive shift of the reduction potentials of oxidants. In the case of Mg^{2+} -catalyzed electron transfer reduction of *p*-benzoquinone derivatives, the formation of 1 : 1 and 1 : 2 complexes between semiquinone radical anion and Mg^{2+} is confirmed by the transient absorption spectra as well as by the ESR spectra. From the spectral change at different Mg^{2+} concentrations is determined the formation constant (K_2) of the 1 : 2 complex. The K_2 values of various semiquinone anions determined from the direct detection of the Mg^{2+} complexes agree well with those estimated from the kinetic analysis on the Mg^{2+} -catalyzed electron transfer reactions. The direct spectroscopic detection of complexes between the semiquinone radical anions and Mg^{2+} , combined with the kinetic analysis of the catalytic effects of Mg^{2+} on not only the electron transfer reactions but also on various reactions involving *p*-benzoquinone derivatives such as Mg^{2+} -catalyzed Diels–Alder reactions of anthracenes with *p*-benzoquinone derivatives, provides a confirmative basis for delineating the catalytic mechanisms of Mg^{2+} on various types of reactions. A remarkable increase in the reactivity of the photoexcited states of carbonyl compounds in the electron transfer reactions is also found by the complexation with Mg^{2+} . The photoexcitation of the Mg^{2+} complex results in strong fluorescence in contrast with the nonfluorescent excited states of uncomplexed carbonyl compounds. Thus, various redox reactions of carbonyl compounds via photoinduced electron transfer are made possible by the catalysis of metal ions which form complexes with carbonyl compounds. The fundamental concept and the scope of catalysis on electron transfer are reviewed in this account to provide some insight into the mechanistic viability.

The importance of electron transfer processes has been recognized in nearly every subdiscipline of chemistry, i.e., not only inorganic chemistry but also organic and organometallic chemistry.¹⁾ Numerous organic reactions, previously formulated by “movements of electron pairs” are now understood as processes in which an initial electron transfer from a nucleophile (reductant) to an electrophile (oxidant) produces a radical ion pair, which leads to the final products via the follow-up steps involving cleavage and formation of chemical bonds.^{2–4)} The follow-up steps are usually sufficiently rapid to render the initial electron transfer the rate-determining step in an overall irreversible transformation. Since photoexcitation induces significant enhancement in the reactivity of electron transfer, photochemical reactions via photoinduced electron transfer have also been explored extensively.^{5,6)} In contrast with the obvious ubiquity of electron transfer processes in photochemical reactions, it has been extremely difficult to distinguish between conventional ionic or concerted mechanisms and electron transfer mechanisms of thermal

redox reactions, although in some cases detection of radical intermediates or isolation of products that could have arisen only via radicals represents good evidence for the electron transfer mechanisms.^{7,8)} If an electron transfer step is the rate-determining step in an overall thermal redox reaction, it would be almost impossible to detect the initial products of electron transfer because of the extremely short lifetimes. Moreover, the final products and kinetics are often the same regardless of the mechanisms. In such cases, the mechanistic distinction seems to be dubious and possibly even meaningless, unless one mechanism provides a more quantitative description of the energetic profiles of the reactions than the other does. Thus, a new approach is certainly required in order to obtain quantitative information about transition states of redox reactions.

This account is intended to focus on catalysis on electron transfer by investigating the effects of an acid or of metal ions introduced as an appropriate third component that can reduce the activation barrier of electron transfer reactions.

The comparison of the catalytic effects of acids and metal ions on electron transfer reactions with those on the redox reactions of the same substrates would provide a valuable quantitative basis to distinguish between conventional ionic or concerted mechanisms and electron transfer mechanisms of thermal redox reactions. More importantly both thermal and photochemical redox reactions which would otherwise be unlikely to occur are made possible to proceed efficiently by the catalysis on the electron transfer steps. First the fundamental concepts of catalysis on electron transfer are presented and then the mechanistic viability is described by showing a number of examples of both thermal and photochemical reactions that involve catalyzed electron transfer processes as the rate-determining steps.

Fundamental Concepts of Catalysis on Electron Transfer. Electron transfer reactions are generally regarded as very fast processes which are in no need of catalysis to accelerate the rates of electron transfer. This is largely true for reversible electron transfer reactions in which electron transfer occurs only when the free energy change of electron transfer is negative, i.e., the electron transfer is exergonic. If the electron transfer is endergonic, no net electron transfer would occur. In the case of irreversible electron transfer when the electron transfer is endergonic but the follow-up reactions are highly exergonic to make the overall redox reactions proceed, however, the initial electron transfer step could be very slow, being the rate-determining step as shown in Fig. 1. In such a case the catalysis on electron transfer would play an essential role in reducing the activation barrier of the overall redox reaction.

According to the Marcus theory,⁹⁾ rates of electron transfer are determined by the free energy change of electron transfer (ΔG_{et}^0) and the reorganization energy associated with the electron transfer (λ). As shown in Fig. 2, an electron is transferred from an electron donor (D) to an acceptor (A) instantaneously according to the Franck–Condon principle when the reactant pair is activated to reach the nuclear configurations which include the solvation, where the energy

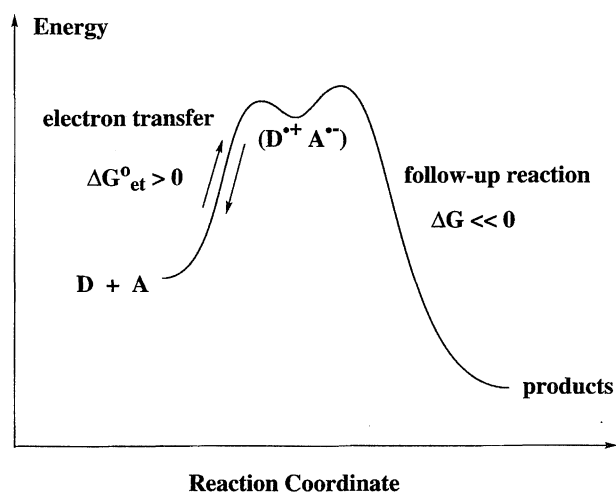


Fig. 1. Energy diagram of irreversible electron transfer from an electron donor (D) to an acceptor (A).

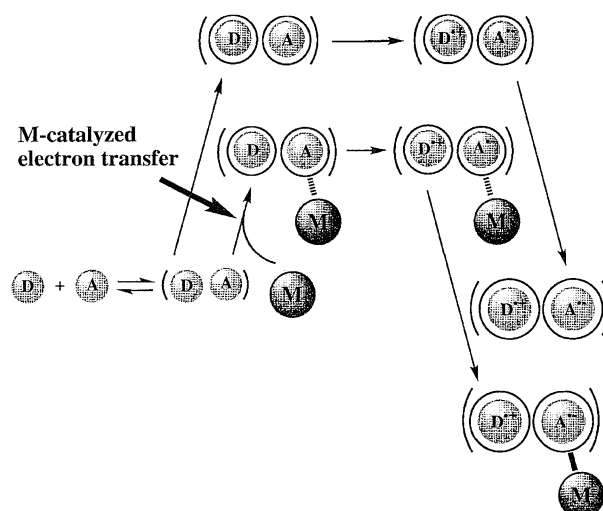
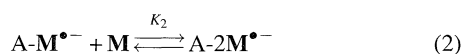


Fig. 2. Catalysis of **M** on an electron transfer process from an electron donor (D) to an acceptor (A).

before and after the electron transfer is the same. If a third component (**M**) which can stabilize one of the products of electron transfer thermodynamically is introduced into the D–A system, the free energy change of electron transfer is shifted to the negative direction, when the activation barrier of electron transfer is reduced to accelerate the rates of electron transfer as shown in Fig. 2, where **M** forms a complex with $A^{\bullet-}$. It should be emphasized that there is no need to have an interaction of **M** with A and that the interaction with the reduced state ($A^{\bullet-}$) is sufficient to accelerate the rate of electron transfer. This contrasts well with the catalysis on conventional ionic or concerted reactions, in which the catalyst needs to interact with a reactant to accelerate the reactions. Since most organic compounds such as π acceptors in particular have small reorganization energies, the change of redox potentials by the interaction of the corresponding radical anions with **M** may be the main factor to accelerate the rates of electron transfer. Thus, any material **M** that can stabilize the radical anions thermodynamically by the complexation may act as an efficient catalyst to accelerate the rates of electron transfer. The stronger the interaction of **M** with their radical anions is, the faster will the rates of electron transfer be as the free energy change of electron transfer decreases. This means that electron is transferred instantaneously according to the Franck–Condon principle when the reactant pair is activated by the unfavorable interaction with **M** to reach the nuclear configurations where the energy before and after the electron transfer is the same. Once an electron is transferred, the interaction of **M** with the radical anion becomes energetically favorable to give the thermodynamically more stable products as shown in Fig. 2.

There may be the case when not only one but also two **M** molecules or ions can interact with $A^{\bullet-}$ as shown in Eqs. 1 and 2. In such a case the one-electron reduction potential of A (E_{red}) may be shifted to the positive direction with an increase in the concentration of **M** according to Eq. 3, which is derived from the Nernst equation of the one-electron

reduction potential in the presence of \mathbf{M} ,¹⁰⁾ where E_{red}^0 is the one-electron reduction potential of A in the absence of \mathbf{M} ,



$$E_{\text{red}} = E_{\text{red}}^0 + (2.3RT/F) \log (1 + K_1[\mathbf{M}] + K_1K_2[\mathbf{M}]^2) \quad (3)$$

K_1 and K_2 are the formation constants of the 1:1 and 1:2 complexes of $\mathbf{A}^{\bullet-}$ with \mathbf{M} , and F is the Faraday constant.

If one assumes that \mathbf{M} has no effect on the oxidation potential of D, the free energy change of electron transfer from D to A in the presence of \mathbf{M} (ΔG_{et}) can be expressed by Eq. 4, where ΔG_{et}^0 is the free energy change in the absence of \mathbf{M} . Thus, electron transfer from D to A becomes more favorable energetically with an increase in the concentration of \mathbf{M} . If such a change in the energetics is directly reflected in the transition state of electron transfer, the dependence of the rate constant of \mathbf{M} -catalyzed electron transfer (k_{et}) on $[\mathbf{M}]$ may be given by Eq. 5, where k_{et}^0 is the rate constant in the absence of \mathbf{M} . Thus, the dependence of the rate constant of \mathbf{M} -catalyzed electron transfer on $[\mathbf{M}]$ is expected to change from the first-order to the second-order with respect to $[\mathbf{M}]$ at the concentration region where $\mathbf{A}^{\bullet-}$ can form the 1:2 complex with \mathbf{M} . The validity of Eq. 5 is confirmed in a number of examples of \mathbf{M} -catalyzed electron transfer reactions (vide infra).

$$\Delta G_{\text{et}} = \Delta G_{\text{et}}^0 - (2.3RT) \log (1 + K_1[\mathbf{M}] + K_1K_2[\mathbf{M}]^2) \quad (4)$$

$$k_{\text{et}} = k_{\text{et}}^0 (1 + K_1[\mathbf{M}] + K_1K_2[\mathbf{M}]^2) \quad (5)$$

Acid Catalysis on Electron Transfer. The simplest substance which can act as a catalyst on electron transfer may be a proton, since radical anions of electron acceptors become stronger bases as compared with the neutral forms. The substrates we first examine are *p*-benzoquinone derivatives (Q), since the redox and acid-base properties of Q and the reduced forms (one-electron and two-electron) have well been established and they exhibit important thermodynamic parameters in biological redox systems.^{11,12)} The variations of the reduction potentials with pH are governed by the acid-base properties of the reduced species. As such, the one-electron reduction potential of Q (E_{red}) is shifted to the positive direction by the protonation of the reduced species (\mathbf{M} is H^+ in Eqs. 1 and 2), according to Eq. 3, where K_1 and K_2 are replaced by K_{a1}^{-1} and K_{a2}^{-1} (K_{a1} and K_{a2} are the acid dissociation constants of QH^{\bullet} and $\text{QH}_2^{\bullet+}$, respectively). At high pH values ($\text{pH} > \text{p}K_{a1}$), $\text{Q}^{\bullet-}$ predominates as the reduced species, and thereby E_{red} is independent of pH, equal to E_{red}^0 . In such a case the rate constant of electron transfer reduction of Q (k_{et}) may be independent of pH. In the region $\text{p}K_{2a} < \text{pH} < \text{p}K_{1a}$, QH^{\bullet} predominates as the reduced species when the E_{red} value is shifted to the positive direction with the slope of $2.3RT/F$ (F is the Faraday constant) which corresponds to 0.0592 at 298 K. In this region the k_{et} value increases linearly with an increase in $[\text{H}^+]$ according to Eq. 5,

where $\mathbf{M} = \text{H}^+$ and $K_{2a}^{-1}[\text{H}^+] \ll 1$. Under more acidic conditions such that $\text{pH} < \text{p}K_{2a}$, the k_{et} value increases showing the second-order dependence on $[\text{H}^+]$ according to Eq. 5, where $K_{2a}^{-1}[\text{H}^+] \gg 1$.

In order to examine the catalysis on electron transfer reduction of Q, one should choose an appropriate electron donor which undergoes irreversible electron transfer oxidation (vide infra). We have previously reported that *cis*-dialkylcobalt(III) complexes, *cis*- $[\text{R}_2\text{Co}(\text{bpy})_2]^+$ (Chart 1; $\text{R} = \text{Me}$, Et, PhCH_2 ; $\text{bpy} = 2,2'$ -bipyridine), undergo facile cleavage of a pair of cobalt-alkyl bonds upon the one-electron oxidation by an oxidant (Scheme 1).¹³⁾ Figure 3 shows the pH dependence of the observed second-order rate constants (k_{et}) of electron transfer from *cis*- $[\text{Et}_2\text{Co}(\text{bpy})_2]^+$ to a series of *p*-benzoquinone derivatives in H_2O -EtOH (5:1 v/v) at 298 K. The $\log k_{\text{et}}$ value of each Q in Fig. 3 exhibits variation with pH, in agreement with that expected from Eq. 5. When a relatively strong oxidant such as 2,6- or 2,5-dichloro-*p*-benzoquinone is employed in the electron transfer oxidation of *cis*- $[\text{Et}_2\text{Co}(\text{bpy})_2]^+$, the k_{et} value is constant, independent of pH at high pH, $\text{pH} > \text{p}K_{1a}$. The acid catalysis starts to operate under acidic conditions, $\text{pH} < \text{p}K_{1a}$ (Fig. 3). Under more acidic conditions such that $\text{pH} < \text{p}K_{2a}$, the slope changes from -1 to -2 showing the second-order dependence of k_{et} on $[\text{H}^+]$, agreeing with the expectation based on Eq. 5. The $\text{p}K_{1a}$ and $\text{p}K_{2a}$ values of each Q determined from the pH dependence of k_{et} agree well with those reported in the literature.¹¹⁾ Thus, the acceleration of rate of electron transfer is achieved by the protonation of the reduced species as shown in Fig. 2 ($\mathbf{M} = \text{H}^+$), and the number of protons which can form the chemical bond with the reduced species determines the kinetic order with respect to the acid concentration. It should be noted that no protonation of Q occurs in the pH region in Fig. 3.

Mechanistic Insight into Acid-Catalyzed Hydride Transfer.

If the electron transfer reduction of Q is the rate-determining step in an overall two-electron reduction process such as hydride reduction of Q, the two-electron reduction process may be subjected to the same catalysis as observed in Fig. 3. Figure 4 shows the pH dependence of the observed second-order rate constants ($\log k_{\text{obs}}$) for the hydride transfer from an acid-stable NADH model compound, 10-methyl-9,10-dihydroacridine (AcrH_2),¹⁴⁾ to Q in H_2O -EtOH

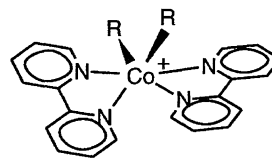
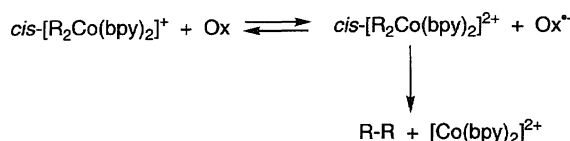


Chart 1.



Scheme 1.

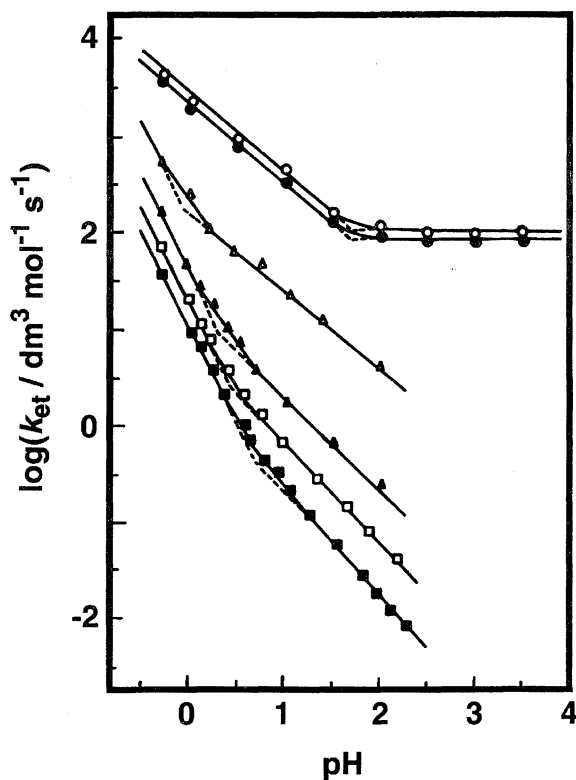


Fig. 3. pH Dependence of k_{et} for the electron transfer from $cis\text{-}[\text{Et}_2\text{Co}(\text{bpy})_2]^+$ to p -benzoquinone derivatives in H_2O - EtOH (5:1 v/v) at 298 K; 2,6-dichloro- p -benzoquinone (\circ), 2,5-dichloro- p -benzoquinone (\bullet), chloro- p -benzoquinone (\triangle), p -benzoquinone (\blacktriangle), methyl- p -benzoquinone (\square), and 2,6-dimethyl- p -benzoquinone (\blacksquare).

(5:1 v/v) at 298 K (Eq. 6).¹⁵ The $\log k_{obs}$ value of each Q in Fig. 4 exhibits variation with pH in agreement with the pH dependence of E_{red} in Eq. 5 as well as the pH dependence of k_{et} of electron transfer from $cis\text{-}[\text{Et}_2\text{Co}(\text{bpy})_2]^+$ to Q in Fig. 3. The $\log k_{obs}$ value of each Q is independent of pH in the region of $\text{pH} > \text{p}K_{1a}$, but increases with decreasing pH in the region $\text{pH} < \text{p}K_{1a}$. The $\text{p}K_{1a}$ values thus determined for various p -benzoquinone derivatives agree well with the literature values.¹¹ In the case of 7,7,8,8-tetracyano- p -quinodimethane (TCNQ), the $\log k_{obs}$ value is independent of pH (Fig. 4), since no protonation of $\text{TCNQ}^{\bullet-}$ has occurred in this pH region. Generally, the easier the reduction of substrate, the more difficult becomes the protonation of the reduced species.

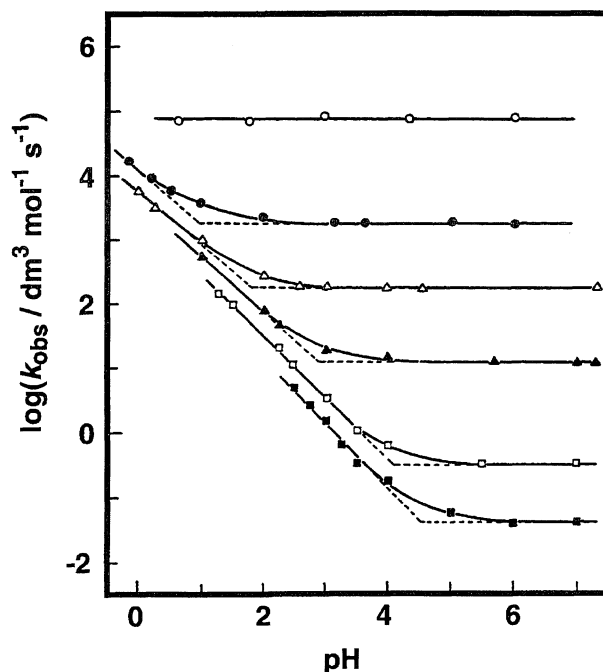
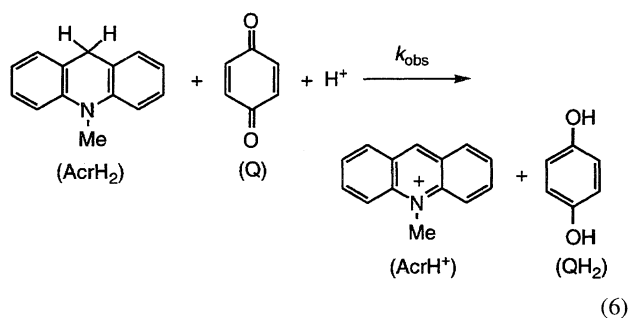
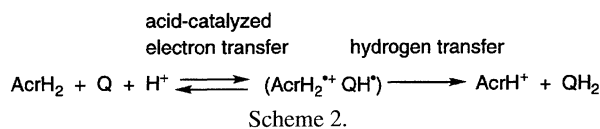


Fig. 4. Plots of $\log k_{obs}$ vs. pH for the hydride transfer reactions from AcrH_2 to TCNQ (\circ), chloranil (\bullet), 2,6-dichloro- p -benzoquinone (\triangle), chloro- p -benzoquinone (\blacktriangle), p -benzoquinone (\square), and methyl- p -benzoquinone (\blacksquare) in H_2O - EtOH (5:1 v/v) at 298 K.

We have previously reported that hydride transfer from NADH model compounds such as AcrH_2 to Q proceeds via electron transfer from AcrH_2 to Q followed by proton transfer from $\text{AcrH}_2^{\bullet+}$ to $\text{Q}^{\bullet-}$ based on the dependence of the observed rate constant on the free energy change of electron transfer as well as the dependence of the kinetic deuterium isotope effects ($k_{\text{H}}/k_{\text{D}}$) on the free energy change of proton transfer from $\text{AcrH}_2^{\bullet+}$ to $\text{Q}^{\bullet-}$.¹⁶ Although a one-step hydride transfer mechanism is sometimes preferred to the electron transfer mechanism,¹⁷ the systematic change of the pH dependence of k_{obs} with a series of p -benzoquinone derivatives in Fig. 4, in agreement with Eq. 5, demonstrates clearly that the initial electron transfer step from AcrH_2 to Q is catalyzed by acid. The pH dependence of the observed kinetic deuterium isotope effects ($k_{\text{H}}/k_{\text{D}}$) also indicates that hydrogen is transferred from $\text{AcrH}_2^{\bullet+}$ to QH^\bullet following the initial electron transfer, as shown in Scheme 2.¹⁸ It should be emphasized here that the question whether the proton is attached before or after the electron transfer is meaningless. Certainly no complete protonation occurs before the electron transfer. If the electron transfer occurs without any interaction of Q with proton and then $\text{Q}^{\bullet-}$ is trapped by proton, no acceleration of the rate of electron transfer would occur. In the region $\text{pH} < \text{p}K_{a1}$, $\text{Q}^{\bullet-}$ is certainly protonated after the electron transfer, but the interaction of Q with the pro-



ton, which is energetically unfavorable, is required before the electron transfer to decrease the energetic barrier of the electron transfer as shown in Fig. 2 ($M=H^+$).

Sextillion Acceleration of Electron Transfer by Acid Catalysis in an Aprotic Solvent. Proton becomes a much stronger acid in an aprotic solvent such as acetonitrile than in water, since the solvation energy for proton in an aprotic solvent is much less than in water.¹⁹⁾ Thus, acid catalysis on electron transfer is expected to be much more efficient in acetonitrile than in water. In fact, the luminescence of $[Ru(bpy)_3]^{2+*}$ is quenched by electron transfer from $[Ru(bpy)_3]^{2+*}$ to acetophenone in the presence of $HClO_4$ in acetonitrile (Eq. 7), although no electron transfer occurs in water.^{12,20)} The k_{et} value increases linearly with the $HClO_4$ concentration ($\leq 0.10 \text{ mol dm}^{-3}$), indicating that one proton is attached to the acetophenone radical anion under such experimental conditions. The luminescence of $[Ru(bpy)_3]^{2+*}$ is quenched also by other acetophenone derivatives having more negative reduction potentials than acetophenone in the presence of $HClO_4$ (0.10 mol dm^{-3}) in acetonitrile at 298 K. Figure 5 shows plots of $\log k_{et}$ values for photoinduced electron transfer from $[Ru(bpy)_3]^{2+*}$ to nitrobenzene derivatives in the absence of $HClO_4$ in acetonitrile²¹⁾ and to acetophenone derivatives in the presence of $HClO_4$ (0.10 mol dm^{-3}) in acetonitrile at 298 K vs. the difference between the one-electron redox potentials of $[Ru(bpy)_3]^{2+*}$ and the electron acceptors in the absence of $HClO_4$, $E_{ox}^0 - E_{red}^0$,

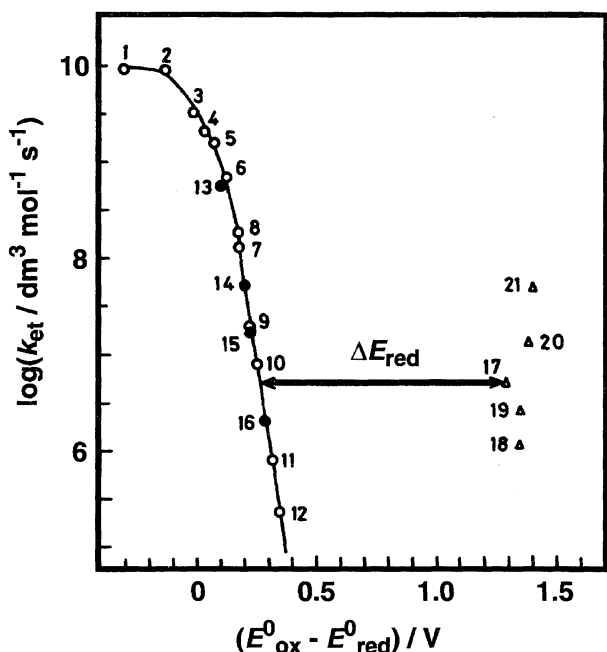
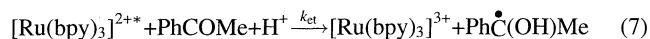
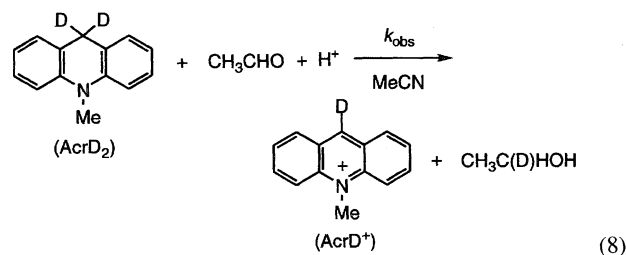


Fig. 5. Plots of $\log k_{et}$ for the photoinduced electron transfer reactions from $[Ru(bpy)_3]^{2+*}$ to organic electron acceptors (Nos. 1–16) in the absence of $HClO_4$ and acetophenone derivatives (Nos. 17–21) in the presence of $HClO_4$ (0.10 mol dm^{-3}) in acetonitrile vs. the difference between the one-electron redox potentials of $[Ru(bpy)_3]^{2+*}$ and the electron acceptors in the absence of $HClO_4$ in acetonitrile, $E_{ox}^0 - E_{red}^0$.

which corresponds to the free energy change of electron transfer, ΔG_{et}^0 .¹²⁾ The dependence of $\log k_{et}$ in the absence of $HClO_4$ on $E_{ox}^0 - E_{red}^0$ is typical for photoinduced electron transfer; the $\log k_{et}$ value increases linearly with decreasing the $E_{ox}^0 - E_{red}^0$ value with the slope of $-F/(2.3RT)$, which is equal to -16.9 at 298 K, to reach the diffusion-limited value, $2.0 \times 10^{10} \text{ dm}^3 \text{ mol}^{-1} \text{ s}^{-1}$.²²⁾ The $\log k_{et}$ values for acetophenone derivatives in the presence of $HClO_4$ (0.10 mol dm^{-3}) are much larger than those extrapolated in the correlation between $\log k_{et}$ and $E_{ox}^0 - E_{red}^0$ (Fig. 5), indicating that the one-electron reduction potentials of acetophenone derivatives are shifted in the positive direction by the presence of $HClO_4$ due to the protonation of the corresponding radical anions. The positive shifts, ΔE_{red} , of acetophenone derivatives in the presence of $HClO_4$ (0.10 mol dm^{-3}) are readily evaluated as the difference in the abscissa between the value on the correlation of $\log k_{et}$ vs. $E_{ox}^0 - E_{red}^0$ and the value in the absence of $HClO_4$ as shown in Fig. 5. The ΔE_{red} value of *p*-methoxyacetophenone in the presence of $0.10 \text{ mol dm}^{-3} HClO_4$ is as large as 1.19 V, which corresponds to a sextillion (10^{21} !) acceleration of the rate of electron transfer at 298 K.



Mechanistic Insight of Acid Catalysis into Biological Redox Systems. In biological redox systems, acid catalysis operates in a hydrophobic environment where the acid strength may be enhanced significantly as compared to that in an aqueous solution. Thus, in the model system, the use of an aprotic solvent may be essential to achieve a high activity of acid catalysis. The enormous enhancement of the rate of electron transfer reduction of carbonyl compounds by acid catalysis in acetonitrile (Fig. 5) is expected to cause a significant decrease in the activation barrier for the two-electron reduction as well, since the subsequent reduction by hydrogen (equivalent to one electron and one proton) following the initial electron transfer is usually highly exergonic. In fact, the two-electron reduction of acetaldehyde, which is the most important substrate with regard to the physiological significance of ethanol metabolism as well as ethanol fermentation,²³⁾ by an acid-stable NADH analogue ($AcrH_2$) is made possible in the presence of $HClO_4$ in acetonitrile.²⁴⁾ When $AcrH_2$ is replaced by the 9,9'-dideuteriated compound, 9,9'-[2H_2]-9,10-dihydro-10-methylacridine ($AcrD_2$), deuterium is introduced to ethanol (Eq. 8).²⁴⁾ Other aliphatic and aromatic ketones as well as aldehydes can also be reduced by $AcrH_2$ in the presence of $HClO_4$ in acetonitrile at 333 K.^{20,24)}



When the k_{et} values of acid-catalyzed photoinduced electron transfer (Eq. 7) are compared with the observed second-order rate constants (k_{obs}) of the acid-catalyzed reduction of aliphatic aldehyde and ketones by AcrH_2 in the presence of HClO_4 , there exists a linear correlation between k_{et} and k_{obs} as shown in Fig. 6.²⁴⁾ The kinetic deuterium isotope effects ($k_{\text{H}}/k_{\text{D}}$) for the acid-catalyzed reduction of aliphatic aldehydes and ketones are uniformly small. For example the $k_{\text{H}}/k_{\text{D}}$ values of acetaldehyde and pivalaldehyde are 1.4 and 1.0, respectively.²⁴⁾ Similar linear correlations between k_{obs} and k_{et} are obtained for aromatic aldehydes and ketones as well.²⁰⁾

Alkylsilanes, which are relatively stable against strong acids as compared with other metal hydrides, have frequently been used as effective hydride donors for the acid-catalyzed reduction of carbonyl compounds.²⁵⁾ Although triethylsilane shows no reactivity toward carbonyl compounds in acetonitrile, the carbonyl compounds are readily reduced by Et_3SiH in the presence of HClO_4 to yield the corresponding alcohol together with a minor amount of the corresponding ether.²⁶⁾ Since the one-electron oxidation potential (E_{ox}^0) of Et_3SiH is higher than 2.3 V (vs. SCE),²⁶⁾ that is significantly higher than the E_{ox}^0 value of AcrH_2 (0.81 V vs. SCE),²⁷⁾ there may be no chance for Et_3SiH acting as an electron donor in the

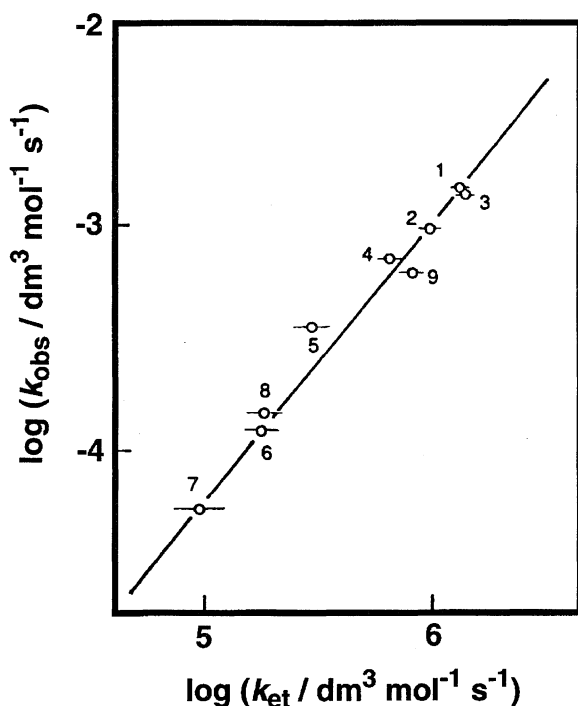


Fig. 6. Plot of $\log k_{\text{obs}}$ for the acid-catalyzed reduction of aldehydes and ketones by AcrH_2 in the presence of HClO_4 ($2.7 \times 10^{-2} \text{ mol dm}^{-3}$) in acetonitrile at 333 K vs. $\log k_{\text{et}}$ for the acid-catalyzed electron transfer from $[\text{Ru}(\text{bpy})_3]^{2+*}$ to the same series of substrates in the presence of HClO_4 (2.0 mol dm^{-3}) at 298 K. Numbers refer to the aldehydes and ketones (1: acetaldehyde, 2: propionaldehyde, 3: butyraldehyde, 4: isovaleraldehyde, 5: isobutyraldehyde, 6: pivalaldehyde, 7: acetone, 8: fluoroacetone, 9: cyclohexanone, 10: pyruvic acid).

acid-catalyzed reduction of carbonyl compounds. Thus, the observed rate constants (k_{obs}) can be used as an authentic reference to know the reactivity of carbonyl compounds in the acid-catalyzed hydride transfer without any contribution from the electron transfer step. In contrast with the case of the acid-catalyzed reduction of carbonyl compounds by AcrH_2 , comparison of the k_{obs} values of Et_3SiH and the k_{et} values of $[\text{Ru}(\text{bpy})_3]^{2+*}$ reveals no apparent parallel relation in the reactivities of carbonyl compounds.²⁶⁾ The reactivity of carbonyl compounds in the acid-catalyzed reduction by Et_3SiH is determined mainly by the protonation ability of the carbonyl compounds, while that in the acid-catalyzed electron transfer is determined by two-reverse effects, i.e., the proton- and electron-acceptor abilities.²⁶⁾ Thus, the linear correlation with the slope of unity in Fig. 6 together with the small $k_{\text{H}}/k_{\text{D}}$ values demonstrates the importance of the acid-catalyzed electron transfer step as the rate-determining activation process in the overall hydride transfer reactions, as shown in the case of *p*-benzoquinone (Scheme 2).

More definitive evidence for the acid-catalyzed electron transfer mechanism is obtained by identifying the products that could arise only via electron transfer processes (vide infra). Remarkable acid catalysis is also observed in thermal electron transfer from mild inorganic one-electron reductants, 1,1'-dimethylferrocene $[\text{Fe}(\text{MeC}_5\text{H}_4)_2]$ and decamethylferrocene $[\text{Fe}(\text{Me}_5\text{C}_5)_2]$ to a series of α -halo ketones such as phenacyl halides (PhCOCH_2X , $\text{X}=\text{Br}, \text{Cl}$) in the presence of HClO_4 in acetonitrile at 335 K (Eq. 9).²⁸⁾ No reaction is observed in the absence of HClO_4 or in the presence of HClO_4 in an aqueous solution. The second-order rate constant of electron transfer (k_{et}) increases linearly with an increase in the HClO_4 concentration. In this case no hydrogen transfer process is involved, and thus the second electron transfer yields the dehalogenated products (Eq. 9), as shown in Table 1. When the one-electron reductants are replaced by AcrH_2 being a hydride donor in the reduction of α -halo ketones, the same dehalogenated products are obtained as in the case of electron transfer reduction, together with the corresponding halo alcohols (Eq. 10).²⁸⁾ The product ratios between ketones and halo-alcohols vary depending on α -halo ketones, as shown in Table 1. When AcrH_2 is replaced by the 9,9'-dideuteriated analogue (AcrD_2), no deuterium is incorporated into acetophenone, but it is introduced to each α -halo alcohol.²⁸⁾

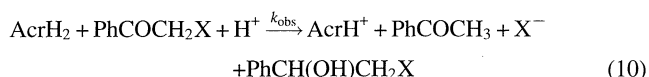
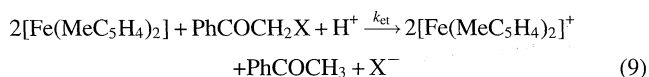
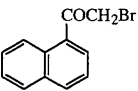
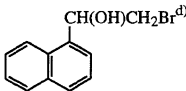
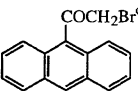
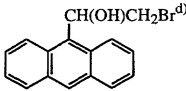
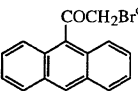
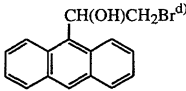


Figure 7 shows comparison of the observed second-order rate constants (k_{obs}) for the acid-catalyzed reduction of various α -halo ketones by AcrH_2 with the rate constants (k_{et}) for the acid-catalyzed thermal electron transfer reactions from ferrocene derivatives and those for the photoinduced electron transfer from $[\text{Ru}(\text{bpy})_3]^{2+*}$ to the same series of α -

Table 1. Acid-Catalyzed Reduction of α -Halo Ketones by AcrH₂, AcrD₂, and [Fe(MeC₅H₄)₂] in the Presence of HClO₄ (0.30 mol dm⁻³) at 335 K

Entry	Substrate ^{a)}	Reductant	Product yield (%) ^{b)}
1	C ₆ H ₅ COCH ₂ Cl	AcrH ₂	C ₆ H ₅ COCH ₃ (36)
	C ₆ H ₅ COCH ₂ Cl	AcrD ₂	C ₆ H ₅ COCH ₃ (57)
	C ₆ H ₅ COCH ₂ Cl ^{c)}	[Fe(MeC ₅ H ₄) ₂]	C ₆ H ₅ COCH ₃ (100)
2	C ₆ H ₅ COCH ₂ Br	AcrH ₂	C ₆ H ₅ COCH ₃ (82)
	C ₆ H ₅ COCH ₂ Br	AcrD ₂	C ₆ H ₅ COCH ₃ (90)
	C ₆ H ₅ COCH ₂ Br	[Fe(MeC ₅ H ₄) ₂]	C ₆ H ₅ COCH ₃ (100)
3	4-MeOC ₆ H ₄ COCH ₂ Br	AcrH ₂	4-MeOC ₆ H ₄ COCH ₃ (48)
	4-MeOC ₆ H ₄ COCH ₂ Br	AcrD ₂	4-MeOC ₆ H ₄ COCH ₃ (72)
	4-MeOC ₆ H ₄ COCH ₂ Br	[Fe(MeC ₅ H ₄) ₂]	4-MeOC ₆ H ₄ COCH ₃ (100)
4	4-MeC ₆ H ₄ COCH ₂ Br	AcrH ₂	4-MeC ₆ H ₄ COCH ₃ (82)
	4-MeC ₆ H ₄ COCH ₂ Br	AcrD ₂	4-MeC ₆ H ₄ COCH ₃ (91)
5	2,4-Cl ₂ C ₆ H ₃ COCH ₂ Br	AcrH ₂	2,4-Cl ₂ C ₆ H ₃ COCH ₃ (84)
6	4-BrC ₆ H ₄ COCH ₂ Br	AcrH ₂	4-BrC ₆ H ₄ COCH ₃ (87)
7	4-(CN)C ₆ H ₄ COCH ₂ Br	AcrH ₂	4-(CN)C ₆ H ₄ COCH ₃ (95)
8	C ₆ H ₅ COCH(Br)C ₂ H ₅	AcrH ₂	C ₆ H ₅ COC ₃ H ₇ (92)
9	C ₆ H ₅ COCH(Br)C ₈ H ₁₇	AcrH ₂	C ₆ H ₅ COC ₉ H ₁₉ (55)
10		AcrH ₂	 (98)
			 (98)
11		AcrH ₂	 (98)

a) The substrate concentration is 0.30 mol dm⁻³ unless otherwise noted. b) The alcohol produced by further reduction of each ketone is not included. c) 0.10 mol dm⁻³. d) Trace amount.

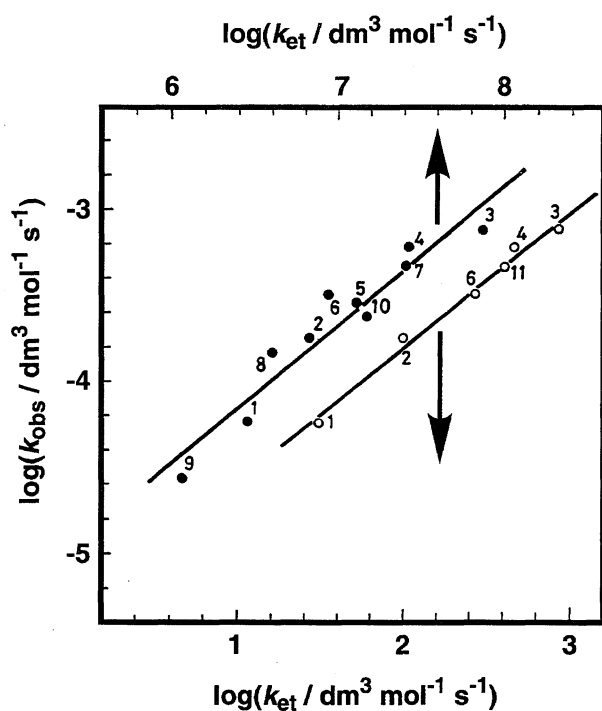
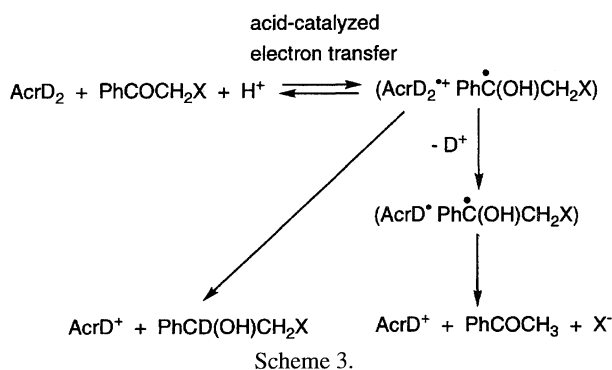


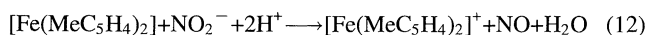
Fig. 7. Plots of $\log k_{\text{obs}}$ for the acid-catalyzed reduction of α -halo ketones by AcrH₂ in the presence of HClO₄ (0.30 mol dm⁻³) in acetonitrile at 335 K vs. $\log k_{\text{et}}$ for the acid-catalyzed electron transfer reactions from [Fe(Me₅C₅)₂] and [Ru(bpy)₃]^{2+*} to α -halo ketones in the presence of HClO₄ (0.30 mol dm⁻³) at 298 K. Numbers refer to α -halo ketones in Table 1.

haloketones.²⁸⁾ There are linear correlations between the k_{obs} values and the k_{et} values, despite the apparent difference in the products between the reduction by a hydride donor (AcrH₂) and electron donors (ferrocene derivatives) as shown in Table 1. Such correlations strongly suggest that the acid-catalyzed reduction of α -haloketones by AcrH₂ to yield the corresponding ketones and α -haloalcohols (Eq. 10) involves a common activation process, i.e., the acid-catalyzed electron transfer from AcrH₂ to α -haloketones as shown in Scheme 3 for the AcrD₂-PhCOCH₂X system. The electron transfer from AcrD₂ to PhCOCH₂X is subject to acid catalysis to generate the radical pair (AcrD₂^{•+} PhC(OH)CH₂X[•]), which disappears either by deuterium (or hydrogen) transfer from AcrD₂^{•+} to PhC(OH)CH₂X[•] or second electron transfer from AcrD₂^{•+}, which is formed by the deprotonation of AcrD₂^{•+}, to PhC(OH)CH₂X[•] as shown in Scheme 3. The deuterium

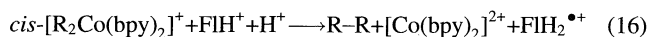
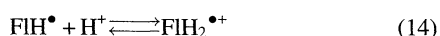


transfer yields $\text{PhCD}(\text{OH})\text{CH}_2\text{X}$, while the second electron transfer yields PhCOCH_3 , accompanied by the reductive dehalogenation (Scheme 3). This may be the reason why the deuterium is incorporated into α -haloalcohol, but not into acetophenone. The observed primary kinetic isotope effects (e.g., $k_{\text{H}}/k_{\text{D}}=3.0$ for PhCOCH_2Br) may be ascribed to the hydrogen transfer process as well as to the deprotonation process (Scheme 3).²⁸⁾ In the case of one-electron reductants (ferrocene derivatives), no hydrogen transfer process is involved and thus the second electron transfer yield only PhCOCH_3 .

Acid-catalyzed electron transfer plays an important role in reduction of not only carbonyl compounds but also other substrates. Both the two-electron reductant (AcrH_2) and one-electron reductant $[\text{Fe}(\text{MeC}_5\text{H}_4)_2]$ can reduce nitrite to nitrogen monoxide in the presence of HClO_4 in acetonitrile at 298 K as shown in Eqs. 11 and 12, respectively.²⁹⁾ In the acid-catalyzed one-electron reduction of nitrite to nitrogen monoxide in acetonitrile containing H_2O , the observed second-order rate constants k_{obs} increase with an increase in the HClO_4 concentration and both k_{obs} values of AcrH_2 and $[\text{Fe}(\text{MeC}_5\text{H}_4)_2]$ show a first-order dependence on $[\text{HClO}_4]$ in the low concentration region, changing to second-order dependence in the higher concentration region.²⁹⁾ The identical change in the order with respect to $[\text{HClO}_4]$ depending on the H_2O concentration may reflect the common activation barrier for the acid-catalyzed electron transfer of the two-electron and one-electron reductants.



Acid catalysis is also effective for the reduction of flavins, which are also important coenzymes in the biological redox reactions, by AcrH_2 in acetonitrile.³⁰⁾ Flavin analogs (Fl, Chart 2) are known to be protonated at the N-1 position in a strongly acidic aqueous solution ($\text{p}K_{\text{a}}=\text{ca. } 0$).³¹⁾ In acetonitrile, the protonation of Fl (Eq. 13) occurs much more readily than in H_2O . The one-electron reduced radical FlH^\bullet can also be protonated to give $\text{FlH}_2^{\bullet+}$ in acetonitrile (Eq. 14). In such a case, the acid catalyzed reduction of Fl by AcrH_2 occurs in acetonitrile to yield AcrH^+ and $\text{FlH}_2^{\bullet+}$ (Eq. 15), although no reaction occurs without acid.³⁰⁾ The acid-catalyzed electron transfer from $\text{cis-}[\text{R}_2\text{Co}(\text{bpy})_2]^+$ to FlH^+ in acetonitrile also occurs to yield $\text{FlH}_2^{\bullet+}$ (Eq. 16).³⁰⁾ The formation of $\text{FlH}_2^{\bullet+}$ is well characterized by the ESR spectra.³⁰⁾ Since



Fl is already protonated at the oxidized state, the rate constant of electron transfer (k_{et}) in such a case increases linearly

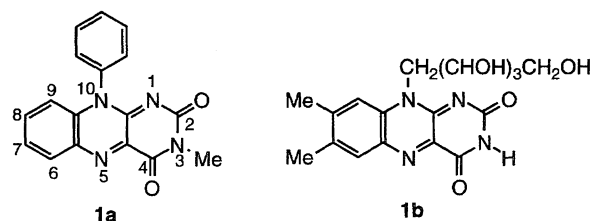
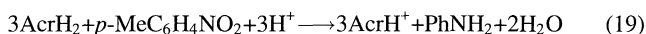


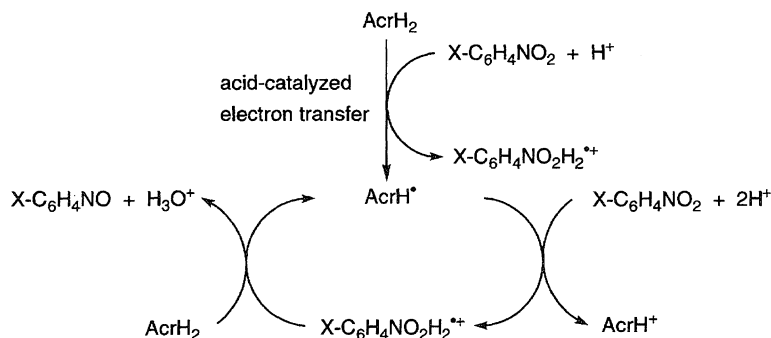
Chart 2.

with $[\text{H}^+]$ in contrast with the case of the acid-catalyzed reduction of Q in Fig. 3, where the k_{et} value shows the second-order dependence with respect to $[\text{H}^+]$ when QH^\bullet is further protonated to give $\text{QH}_2^{\bullet+}$.

Acid-Catalyzed Multi-Electron Reduction. The acid catalysis observed in the one-electron and two-electron reduction of substrates described above is also effective for multi-electron reduction of nitrobenzene derivatives.³²⁾ Nitrobenzene (PhNO_2) is readily reduced by AcrH_2 in the presence of HClO_4 in acetonitrile at 313 K to yield the four-electron reduction product, *N*-phenylhydroxylamine (PhNHOH) as shown in Eq. 17.³²⁾ The two-electron reduction of nitrosobenzene (PhNO) by AcrH_2 in the presence of HClO_4 in acetonitrile also occurs to yield PhNHOH (Eq. 18) with the much faster rate at a lower temperature (298 K) than the four-electron reduction of PhNO_2 . Thus, the rate-determining step of the four-electron reduction of nitrobenzene may be the two-electron reduction of PhNO_2 to PhNO .³²⁾ When *p*-nitrotoluene is used as a substrate, the acid-catalyzed reduction by AcrH_2 yields the six-electron reduction product, i.e., *p*-methylaniline (Eq. 19).³²⁾



Based on the observation of chemically induced dynamic nuclear polarization (CIDNP) in the ^1H NMR spectra of the reactants during the reaction, the unusual kinetics showing the one-half order dependence of the rate on the AcrH_2 concentration, and the inhibition effect of oxygen, the reaction mechanism for the acid-catalyzed multi-electron reduction of nitrobenzene derivatives by AcrH_2 is revealed to be radical chain reactions shown in Scheme 4.³²⁾ The initiation step is acid-catalyzed electron transfer from AcrH_2 to $\text{X-C}_6\text{H}_4\text{NO}_2$, when two protons are incorporated into the reduced product to yield $\text{X-C}_6\text{H}_4\text{NO}_2\text{H}_2^{\bullet+}$. The acid catalysis on the electron transfer reduction of nitrobenzene has been examined by the acid-catalyzed photoinduced electron transfer from $[\text{Ru}(\text{bpy})_3]^{2+*}$ to nitrobenzene in acetonitrile.³²⁾ Although little quenching of the emission of $[\text{Ru}(\text{bpy})_3]^{2+*}$ is observed by nitrobenzene in acetonitrile, the presence of HClO_4 significantly accelerates the electron transfer from $[\text{Ru}(\text{bpy})_3]^{2+*}$ to nitrobenzene as the case for the acid-catalyzed electron transfer from $[\text{Ru}(\text{bpy})_3]^{2+*}$ to carbonyl compounds in Fig. 5.¹²⁾ The k_{et} value for the photoinduced electron transfer from $[\text{Ru}(\text{bpy})_3]^{2+*}$ to nitrobenzene increases parabolically with

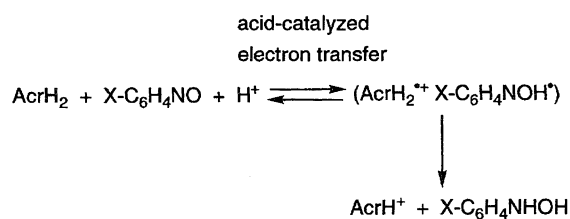


Scheme 4.

an increase in $[\text{HClO}_4]$. The propagation step consists of two redox reactions; one is hydrogen transfer from AcrH_2 to $\text{X-C}_6\text{H}_4\text{NO}_2\text{H}_2^{\bullet+}$ to give AcrH^\bullet and $\text{X-C}_6\text{H}_4\text{NO}$ after dehydration, and the other is the acid-catalyzed electron transfer from AcrH^\bullet to $\text{X-C}_6\text{H}_4\text{NO}_2$ to yield AcrH^+ accompanied by regeneration of $\text{X-C}_6\text{H}_4\text{NO}_2\text{H}_2^{\bullet+}$ (Scheme 4). The observation of large kinetic deuterium isotope effects ($k_{\text{H}}/k_{\text{D}}=6.8$ for nitrobenzene) indicates that hydrogen transfer from AcrH_2 to $\text{X-C}_6\text{H}_4\text{NO}_2\text{H}_2^{\bullet+}$ is the rate-determining step in the chain propagation.³²⁾ Since the chain carrier radical (AcrH^\bullet) is known to be readily trapped by oxygen,^{33,34)} oxygen can act as a strong inhibitor for the radical chain reactions in Scheme 4. It is interesting to note that such strong oxygen inhibition is in fact recognized as the most unique characteristic of nitroreductase.³⁵⁾ The termination step may be the back electron transfer from $\text{X-C}_6\text{H}_4\text{NO}_2\text{H}_2^\bullet$ to $\text{AcrH}_2^{\bullet+}$, which causes the nuclear polarization in the reactants as shown in Eq. 20, where * denotes the nuclear polarization. The strong emission observed for the ortho protons of $\text{X-C}_6\text{H}_4\text{NO}_2$ agrees with that expected from Kaptein's rule.³⁶⁾ The reaction mechanism in Scheme 4 has been well supported by the kinetic analysis of the reaction.³²⁾ The two-electron reduction product, $\text{X-C}_6\text{H}_4\text{NO}$, is further reduced by AcrH_2 via acid-catalyzed electron transfer from AcrH_2 to $\text{X-C}_6\text{H}_4\text{NO}$, followed by hydrogen transfer from $\text{AcrH}_2^{\bullet+}$ to $\text{X-C}_6\text{H}_4\text{NOH}^\bullet$, yielding the corresponding four-electron reduction product, $\text{X-C}_6\text{H}_4\text{NHOH}$ as shown in Scheme 5. When an appropriate substituent is introduced at the para position, the four electron reduced product $p\text{-X-C}_6\text{H}_4\text{NHOH}$ (e.g., X=Me) is further reduced by AcrH_2 to yield the corresponding six-electron reduction product, $p\text{-X-C}_6\text{H}_4\text{NH}_2$.³²⁾



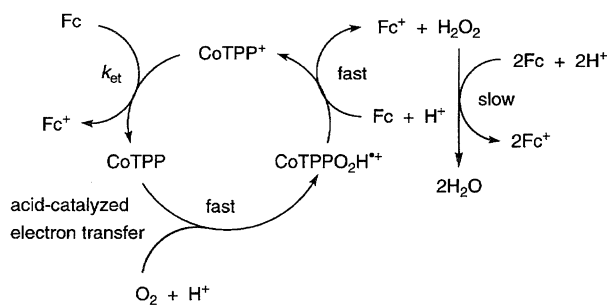
Acid Catalysis on Electron Transfer in the Overall "Catalytic" Cycle. I have demonstrated that acid catalysis on electron transfer from NADH analogs to substrates in



Scheme 5.

aprotic media plays an essential role in reducing the activation barrier for the two-electron and multi-electron reduction of substrates. By using such a simple acid catalyzed system, various NADH-dependent substrates, which would otherwise be activated only by the action of appropriate enzymes, are shown to be readily reduced by an acid-stable NADH analogue. On the other hand, NADH plays a vital role as the electron source in the respiratory chain where the four-electron reduction of dioxygen by NADH is achieved by the step-by-step transfer of electrons through a number of electron carriers such as the cytochromes.^{37,38)} The NADH and analogs are stable against dioxygen showing no direct interaction. Thus, we want to construct more efficient electron transfer catalytic systems for the reduction of dioxygen in the homogeneous systems (vide infra).

Although cobalt(II) tetraphenylporphyrin (CoTPP) cannot reduce dioxygen in acetonitrile, efficient electron transfer from CoTPP to O_2 occurs in the presence of acid. The rate constants of outer-sphere electron transfer from CoTPP to O_2 in the presence of HClO_4 in acetonitrile at 298 K can be calculated by applying the Marcus theory of electron transfer.^{9,39)} The observed rate constants of electron transfer are 10^9 -fold larger than the calculated rate constants.³⁹⁾ The huge enhancement of the observed rates relative to the calculated ones of the outer-sphere electron transfer indicates a strong inner-sphere character in the acid-catalyzed electron transfer from CoTPP to O_2 . Such a strong inner-sphere nature suggests that the electron transfer gives a complex, $\text{CoTPPO}_2\text{H}^{\bullet+}$, in which a strong interaction between CoTPP^+ and HO_2^\bullet causes a significant decrease in the free energy change of acid-catalyzed electron transfer from CoTPP to O_2 .³⁹⁾ On the other hand, electron transfer from ferrocene derivatives (Fc) to CoTPP^+ occurs through the outer-sphere pathway, since the observed rate constants agree well with those calculated by using the Marcus theory of outer-sphere electron transfer.³⁹⁾ The combination of an outer-sphere electron transfer from Fc to CoTPP^+ with an acid-catalyzed inner-sphere electron transfer from CoTPP to O_2 constitutes an efficient catalytic cycle for the reduction of O_2 by Fc, as shown in Scheme 6.³⁹⁾ The further two-electron reduction of H_2O_2 by Fc occurs to yield H_2O , although this process is much slower than the initial two-electron reduction of O_2 . The inner-sphere nature in the acid-catalyzed electron transfer from CoTPP to O_2 is essential to constitute the catalytic cycle. Otherwise CoTPP^+ would only act as an electron mediator and no accel-

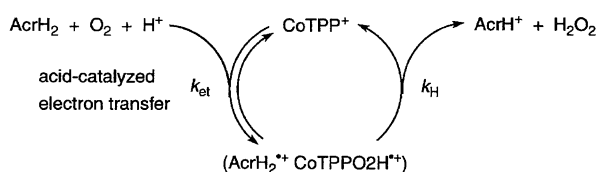


Scheme 6.

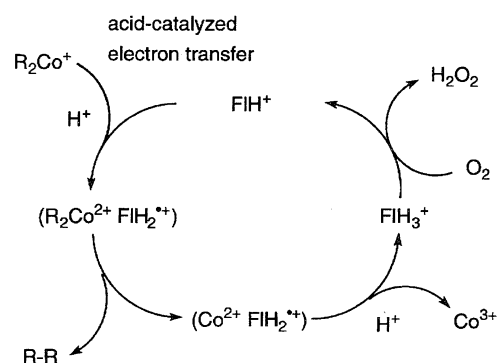
eration of the overall electron transfer from Fc to O₂ would be achieved. Other metalloporphyrins (FeTPP⁺ and MnTPP⁺) can also act as efficient catalysts for the reduction of O₂ by Fc in the presence of HClO₄ in acetonitrile.³⁹⁾

When the one-electron reductant Fc is replaced by an NADH analogue (AcrH₂), electron transfer from AcrH₂ to CoTPP⁺ occurs in concert with the reduction of O₂ by CoTPP in the presence of HClO₄, as shown in Scheme 7.⁴⁰⁾ Electron transfer from AcrH₂ to CoTPP⁺ in the presence of HClO₄ produces a radical pair (AcrH₂^{•+} CoTPPO₂H^{•+}), which disappears by the facile hydrogen transfer from AcrH₂^{•+} to CoTPPO₂H^{•+} to yield AcrH⁺ and H₂O₂, accompanied by regeneration of CoTPP⁺ (Scheme 7). The observed kinetic deuterium isotope effect ($k_H/k_D=7.1$) is ascribed to that of the hydrogen transfer step.⁴⁰⁾ In the case of CoTPP⁺-catalyzed reduction of O₂ by Fc (Scheme 6), the outer-sphere electron transfer from Fc to CoTPP⁺ is the rate-determining step and thereby the rate is independent of acid and O₂ concentrations.³⁹⁾ In contrast, the rate of CoTPP⁺-catalyzed reduction of O₂ by AcrH₂ (Scheme 7) increases linearly with an increase in the acid or O₂ concentration, since the electron transfer from AcrH₂ to CoTPP⁺ and acid-catalyzed electron transfer from CoTPP to O₂ occurs in a concerted manner.⁴⁰⁾

Acid catalysis on electron transfer also plays an essential role in oxygenation and oxidative coupling of alkyl ligands of *cis*-dialkylcobalt(III) complexes with O₂, "catalyzed" by coenzyme analogues in the presence of acid.⁴¹⁾ The overall catalytic cycle for the FIH⁺-catalyzed oxidative coupling of alkyl ligands of *cis*-[R₂Co(bpy)₂]⁺ (R=Me, Et) is shown in Scheme 8, where acid-catalyzed electron transfer from *cis*-[R₂Co(bpy)₂]⁺ (R₂Co⁺) to FIH⁺ occurs to give the corresponding dialkylcobalt(IV) complex (R₂Co²⁺) and FIH₂^{•+}, followed by the facile reductive elimination of the alkyl ligands to yield the coupling product R-R.⁴¹⁾ Then acid-catalyzed electron transfer from the resulting cobalt(II) complex to FIH₂^{•+} occurs to give Co³⁺ and a protonated dihydroflavin FIH₃⁺. The FIH₃⁺ is oxidized by O₂ to regenerate the oxidized protonated form (FIH⁺) accompanied by the formation of



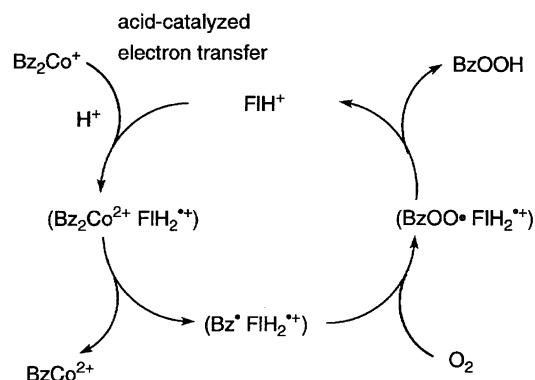
Scheme 7.



Scheme 8.

H₂O₂. In the absence of a coenzyme analogue, the cobalt-carbon bond of *cis*-[R₂Co(bpy)₂]⁺ in both absence and presence of O₂ is cleaved by the electrophilic attack of proton to yield [RCo(bpy)₂]²⁺ and RH.⁴¹⁾ The rates of FIH⁺-catalyzed oxygenation of *cis*-[R₂Co(bpy)₂]⁺ increase linearly with increasing in the concentrations of both HClO₄ and FI.⁴¹⁾

The product in the coenzyme-catalyzed oxidation of *cis*-[R₂Co(bpy)₂]⁺ by O₂ in the case of R=PhCH₂ (Bz₂Co⁺) is drastically changed from R-R in the case of R=Me and Et (Scheme 8) to the oxygenated product BzOOH as shown in Scheme 9.⁴¹⁾ The initial acid-catalyzed electron transfer from Bz₂Co⁺ to FIH⁺ occurs to give Bz₂Co²⁺ and FIH₂^{•+}. The cleavage of cobalt-benzyl bond of Bz₂Co²⁺ occurs in a stepwise manner and the benzyl radical formed is stable enough to be trapped by O₂ to give benzylperoxyl radical (BzOO[•]), which is reduced by hydrogen transfer from FIH₂^{•+} to yield benzyl hydroperoxide, accompanied by regeneration of FIH⁺ (Scheme 9). The benzyl hydroperoxide decomposes to yield the final oxygenated product, benzaldehyde.⁴²⁾ In the absence of O₂, the benzyl radical reacts with [PhCH₂Co(bpy)₂]²⁺ in the cage to yield the coupling product, PhCH₂CH₂Ph. In the case of *cis*-[R₂Co(bpy)₂]⁺ (R=Me, Et) as well, the cleavage of the Co-R bond in *cis*-[R₂Co(bpy)₂]²⁺ may occur in a stepwise manner. However, the reaction of R[•] with [RCo(bpy)₂]²⁺ may be so fast that R[•] cannot be trapped by oxygen and that only the net coupling of the alkyl ligands can occur to yield the coupling products in the presence of O₂. Thus, *cis*-[(PhCH₂)₂Co(bpy)₂]⁺ is the least reactive in the electron transfer oxidation in the absence of O₂ because of the slow coupling process, but it becomes the most reactive

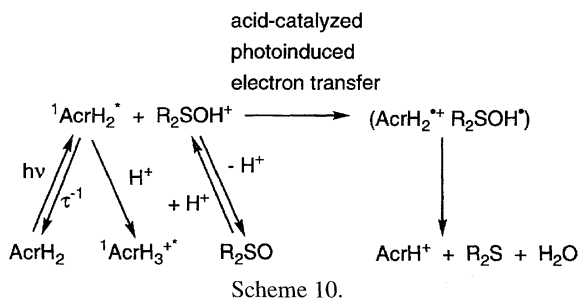


Scheme 9.

in the FlH^+ -catalyzed oxidation by O_2 because of the facile trapping of the benzyl radical by O_2 .⁴¹⁾ Essentially the same reaction schemes (Schemes 8 and 9) are applied for other redox coenzyme analogues such as lumazine and aminopterin which act as catalysts in the oxidation of $\text{cis-}[\text{R}_2\text{Co}(\text{bpy})_2]^+$ by O_2 in the presence of acid.⁴¹⁾

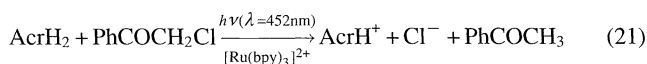
Acid Catalysis in Photochemical Reactions via Photoinduced Electron Transfer. The electron donor and acceptor abilities of electron donors and acceptors are enhanced significantly by the photoexcitation compared to those of the ground states, since the one-electron redox potentials of the excited states are shifted drastically by the photoexcitation.⁵⁾ Since the magnitude of the excitation energy is usually as large as 2–3 eV, the free energy change of photoinduced electron transfer becomes energetically much more favorable owing to the photoexcitation. Thus, the combination of acid catalysis and photoexcitation would expand further the scope of photoinduced electron transfer reactions. For example, the use of the excited state of AcrH_2 combined with acid catalysis makes it possible to reduce dimethyl sulfoxide (Me_2SO) and other dialkyl sulfoxides by AcrH_2 to yield AcrH^+ and the corresponding dialkyl sulfides (R_2S).⁴³⁾ Although a number of substrates can be reduced by AcrH_2 photochemically^{44,45)} or by acid catalysis,^{28–30,32)} neither thermal acid catalysis nor the use of the excited states of NADH analogues is effective for the reduction of Me_2SO , which is commonly used as an inert solvent.

In the presence of HClO_4 (79%, 0.20 mol dm^{-3}), both AcrH_2 and R_2SO are readily protonated in acetonitrile.^{46,47)} The protonation of R_2SO is expected to enhance the electron acceptor ability, while that of AcrH_2 results in a significant decrease in the reducing ability. When H_2O (0.50 mol dm^{-3}) is added to the acetonitrile solution, however, only R_2SO is protonated, while no protonation of AcrH_2 takes place.⁴³⁾ Under such experimental conditions, photoinduced electron transfer from the singlet excited state of AcrH_2 ($^1\text{AcrH}_2^*$) to R_2SOH^+ occurs efficiently to give the radical pair ($\text{AcrH}_2^{\bullet+}$, $\text{R}_2\text{SOH}^\bullet$), as shown in Scheme 10.⁴³⁾ The hydrogen transfer from $\text{AcrH}_2^{\bullet+}$ to $\text{R}_2\text{SOH}^\bullet$ is accompanied by the dehydration of $\text{R}_2\text{SH}(\text{OH})$ to yield AcrH^+ and R_2S (Scheme 10).⁴³⁾ The initial photoinduced electron transfer may be the rate-determining step, since no kinetic deuterium isotope effects have been observed in the overall quantum yields.⁴³⁾ The catalytic function of acid in the photoreduction of R_2SO by AcrH_2 is attributed to the protonation of the ground state-substrate, which enhances the electron transfer from $^1\text{AcrH}_2^*$



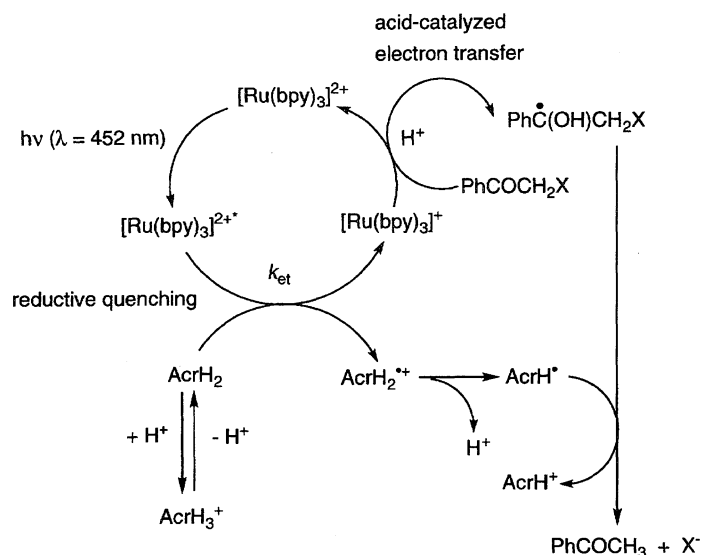
significantly. At the same time, however, the quenching of $^1\text{AcrH}_2^*$ by H^+ reduces the lifetime of $^1\text{AcrH}_2^*$.⁴³⁾ Thus, the concentration of acid should be optimized in order to achieve the high efficiency of the acid-catalyzed photoreduction.

As shown in Eq. 10, the reduction of phenacyl bromide by AcrH_2 occurs thermally in the presence of HClO_4 in acetonitrile at 333 K.²⁸⁾ In the absence of HClO_4 , no reduction of phenacyl bromide by AcrH_2 has occurred thermally. Irradiation of the absorption band due to AcrH_2 in the presence of phenacyl halides (PhCOCH_2X , $\text{X}=\text{Br}$, Cl), however, results in the reductive dehalogenation of PhCOCH_2X to yield AcrH^+ and PhCOCH_3 via photoinduced electron transfer from $^1\text{AcrH}_2^*$ to PhCOCH_2X .⁴⁸⁾ In this case, the excitation of AcrH_2 requires UV or near-UV irradiation ($\lambda_{\text{max}}=285$ nm). However, the use of a photosensitizer, $[\text{Ru}(\text{bpy})_3]^{2+}$, makes it possible to utilize visible light to initiate reaction.⁴⁹⁾ Thus, the addition of $[\text{Ru}(\text{bpy})_3]^{2+}$ to the AcrH_2 – PhCOCH_2Br system and selective irradiation of the absorption band due to $[\text{Ru}(\text{bpy})_3]^{2+}$ ($\lambda_{\text{max}}=452$ nm) results in the formation of AcrH^+ and PhCOCH_3 .⁵⁰⁾ No photochemical reaction has been observed in the absence of $[\text{Ru}(\text{bpy})_3]^{2+}$ under otherwise the same experimental conditions. The concentration of $[\text{Ru}(\text{bpy})_3]^{2+}$ remains unchanged during the photochemical reaction. Thus, $[\text{Ru}(\text{bpy})_3]^{2+}$ acts as a photosensitizer in the photoreduction of PhCOCH_2Br by AcrH_2 , yielding the same products as in the case of direct excitation of the absorption band due to AcrH_2 . In this case, no $[\text{Ru}(\text{bpy})_3]^{2+}$ -sensitized photoreduction of PhCOCH_2Cl by AcrH_2 has occurred. The presence of HClO_4 , however, makes it possible to reduce PhCOCH_2Cl in the $[\text{Ru}(\text{bpy})_3]^{2+}$ -sensitized reaction with AcrH_2 (Eq. 21).⁵⁰⁾



The effect of HClO_4 on the $[\text{Ru}(\text{bpy})_3]^{2+}$ -sensitized reduction of PhCOCH_2Br by AcrH_2 is not straightforward as shown in Fig. 8, which exhibits a complex dependence of Φ on the HClO_4 concentration. The Φ value increase with an increase in the HClO_4 concentration but decreases through a maximum with a further increase in the HClO_4 concentration. In the high concentrations (see the logarithm scale in Fig. 8), the Φ value increases again with an increase in the HClO_4 concentration. Such a bizarre dependence of Φ on $[\text{HClO}_4]$ can be explained by the change of the quenching mechanism from the reductive quenching of $[\text{Ru}(\text{bpy})_3]^{2+*}$ to the oxidative quenching at the high HClO_4 concentrations (vide infra).

In the absence of HClO_4 , the reductive quenching of $[\text{Ru}(\text{bpy})_3]^{2+*}$ by AcrH_2 occurs efficiently by electron transfer from AcrH_2 ($E_{\text{ox}}^0=0.81$ V)²¹⁾ to $[\text{Ru}(\text{bpy})_3]^{2+*}$ ($E_{\text{red}}^0=0.81$ V)²¹⁾ to produce $\text{AcrH}_2^{\bullet+}$ and $[\text{Ru}(\text{bpy})_3]^+$ as shown in Scheme 11. Since $[\text{Ru}(\text{bpy})_3]^+$ is a strong reductant ($E_{\text{ox}}^0=-1.29$ V),²¹⁾ phenacyl bromide and *para*-substituted phenacyl bromides can be readily reduced by $[\text{Ru}(\text{bpy})_3]^+$ to yield the corresponding acetophenone derivatives (Scheme 11). However, phenacyl chloride, which is a much weaker oxidant than phenacyl bromide cannot be re-



Scheme 11.

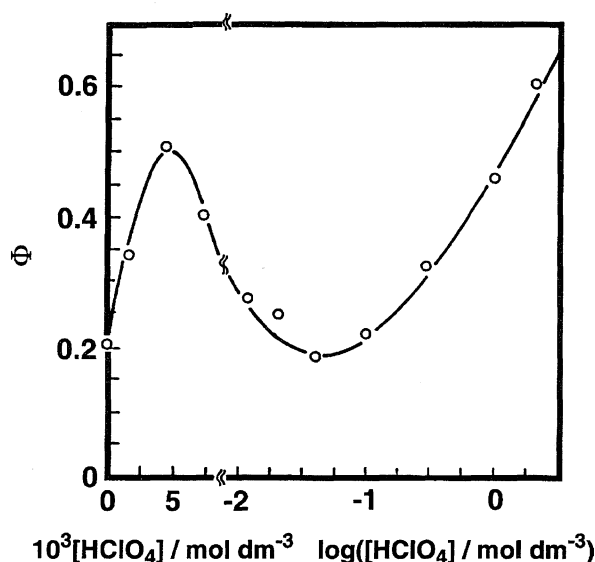
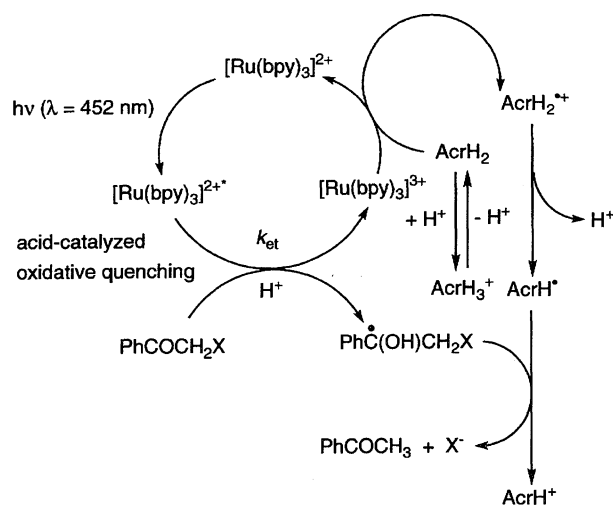


Fig. 8. Plot of the quantum yield Φ vs. the HClO_4 concentration for the $[\text{Ru}(\text{bpy})_3]^{2+}$ -photosensitized reduction of phenacyl bromide ($1.0 \times 10^{-2} \text{ mol dm}^{-3}$) by AcrH_2 ($1.0 \times 10^{-2} \text{ mol dm}^{-3}$) in acetonitrile under irradiation of the visible light $\lambda = 452 \text{ nm}$.

duced by $[\text{Ru}(\text{bpy})_3]^+$ and thus no $[\text{Ru}(\text{bpy})_3]^{2+}$ -sensitized reduction of phenacyl chloride occurs in the absence of HClO_4 . In the presence of HClO_4 , the reductive quenching of $[\text{Ru}(\text{bpy})_3]^{2+*}$ by AcrH_2 may be followed by acid-catalyzed electron transfer from $[\text{Ru}(\text{bpy})_3]^+$ to PhCOCH_2X to give $\text{PhC}(\text{OH})\text{CH}_2\text{X}^\bullet$, accompanied by regeneration of $[\text{Ru}(\text{bpy})_3]^{2+}$, in competition with the back electron transfer from $[\text{Ru}(\text{bpy})_3]^+$ to $\text{AcrH}_2^{\bullet+}$ (Scheme 11).⁵⁰ Thus, the initial increase of Φ with an increase in $[\text{HClO}_4]$ in Fig. 8 is ascribed to the acid catalysis on electron transfer from $[\text{Ru}(\text{bpy})_3]^+$ to PhCOCH_2X . The $\text{AcrH}_2^{\bullet+}$ radical may be deprotonated to give AcrH^\bullet which can reduce $\text{PhC}(\text{OH})\text{CH}_2\text{X}^\bullet$ to yield AcrH^+ and PhCOCH_3 (Scheme 11). The hydrogen in the reduced acetophenone comes from a proton

and thereby replacement of AcrH_2 by AcrD_2 or $\text{AcrH}_2\text{-CD}_3$ results in no incorporation of deuterium into acetophenone.⁵⁰ No kinetic isotope effect is observed, either, since the rate-determining step involves only an electron transfer process, the reductive quenching of $[\text{Ru}(\text{bpy})_3]^{2+*}$ by AcrH_2 or electron transfer from $[\text{Ru}(\text{bpy})_3]^+$ to PhCOCH_2X .⁴⁵ On the other hand, the rate constant of photoinduced electron transfer from AcrH_2 to $[\text{Ru}(\text{bpy})_3]^{2+*}$ decreases with an increase in the HClO_4 concentration because of the protonation of AcrH_2 , resulting in the change of the rate-determining step from the reduction of PhCOCH_2X by $[\text{Ru}(\text{bpy})_3]^+$ to the initial photoinduced electron transfer. This is the reason why the Φ value decreases with an increase in the HClO_4 concentration (5.0×10^{-3} — $4.0 \times 10^{-2} \text{ mol dm}^{-3}$ in Fig. 8).

In the high concentrations of HClO_4 , the $[\text{Ru}(\text{bpy})_3]^{2+}$ -sensitized reactions are started by the oxidative quenching of $[\text{Ru}(\text{bpy})_3]^{2+*}$ by acid-catalyzed electron transfer from $[\text{Ru}(\text{bpy})_3]^{2+*}$ to PhCOCH_2X instead of the reductive quenching by AcrH_2 , as shown in Scheme 12. In fact, the emission of $[\text{Ru}(\text{bpy})_3]^{2+*}$ is quenched by acid-catalyzed electron

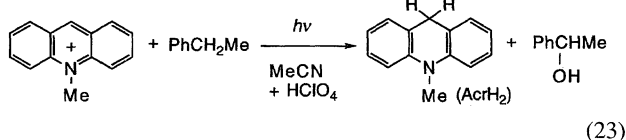
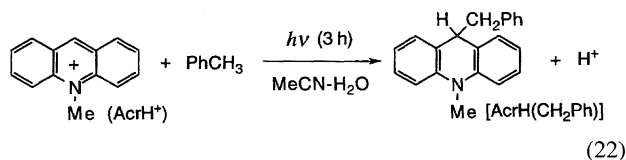


Scheme 12.

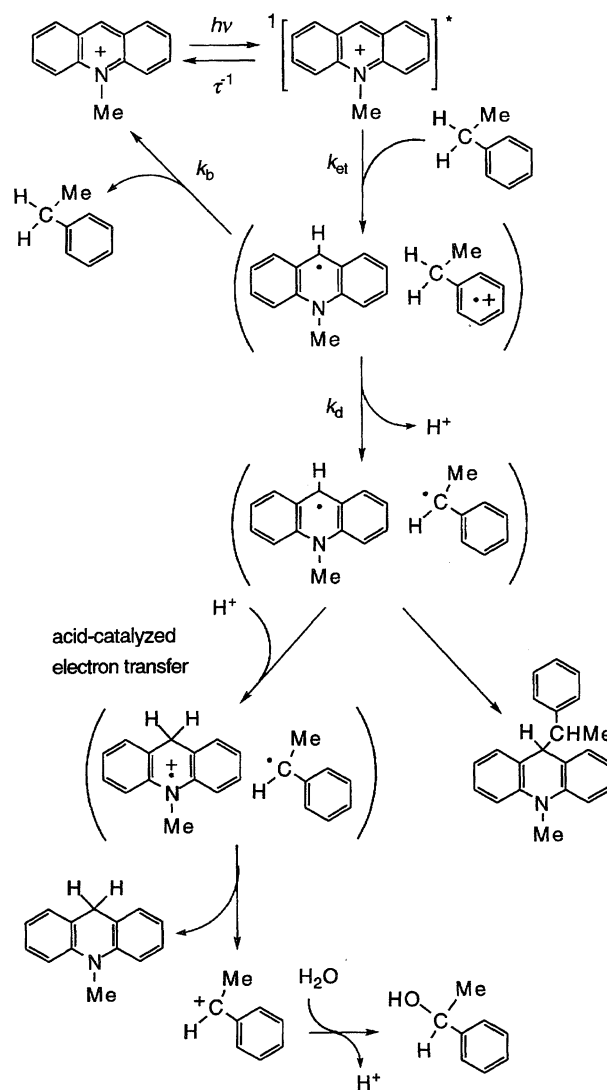
transfer from $[\text{Ru}(\text{bpy})_3]^{2+*}$ to PhCOCH_2X at the high concentrations of HClO_4 , although no oxidative quenching by PhCOCH_2X has occurred in the absence of HClO_4 or at the low concentrations.⁵⁰ Since the rate constant of the reductive quenching of $[\text{Ru}(\text{bpy})_3]^{2+*}$ by AcrH_2 decreases with an increase in the HClO_4 concentration (vide supra), the oxidative quenching becomes a predominant pathway at the high HClO_4 concentrations. This is the reason why the Φ value increases again in the high concentrations of HClO_4 in Fig. 8. The acid-catalyzed oxidative quenching of $[\text{Ru}(\text{bpy})_3]^{2+*}$ by PhCOCH_2X produces $\text{PhC}(\text{OH})\text{CH}_2\text{X}^\bullet$ and $[\text{Ru}(\text{bpy})_3]^{3+}$. Since $[\text{Ru}(\text{bpy})_3]^{3+}$ is a very strong oxidant ($E_{\text{red}}^0 = 1.3 \text{ V}$),²¹ AcrH_2 can be oxidized even in the presence of HClO_4 to produce $\text{AcrH}_2^{\bullet+}$, accompanied by regeneration of $[\text{Ru}(\text{bpy})_3]^{2+}$ (Scheme 12). The $\text{AcrH}_2^{\bullet+}$ is oxidized by $\text{PhC}(\text{OH})\text{CH}_2\text{X}^\bullet$ to yield the same products as the case in Scheme 11.

As shown above, the acid catalysis on electron transfer increases the overall efficiency of the photochemical reactions via photoinduced electron transfer without affecting the products. On the other hand, there is a case when the acid catalysis on a particular electron transfer process results in a drastic change of the products in the overall photochemical reactions (vide infra).

It has been demonstrated that visible light irradiation of the absorption band of 10-methylacridinium ion (AcrH^+) in the presence of organometallic compounds, alkenes and alkylbenzenes in acetonitrile results in efficient C–C bond formation between these electron donors and AcrH^+ via photoinduced electron transfer from the donors to the singlet excited state of AcrH^+ to yield the alkylated or allylated adducts selectively.^{51,52} The AcrH^+ is also photoreduced by ethylbenzene and other alkylbenzenes to yield the corresponding 9-substituted-10-methyl-9,10-dihydroacridine, as shown in Eq. 22.⁵³ In the presence of HClO_4 (1.2 mol dm^{-3}), however, the photooxygenation of ethylbenzene to 1-phenylethanol occurs as shown in Eq. 23, where AcrH^+ is reduced to 10-methyl-9,10-dihydroacridine (AcrH_2) instead of the adduct.⁵⁴ In the case of the other alkylbenzenes such as cumene and diphenylmethane, the photoinduced hydride reduction of AcrH^+ to AcrH_2 occurs in the presence of HClO_4 , accompanied by the oxygenation of alkylbenzenes to the corresponding benzyl alcohol. When the HClO_4 concentration is reduced from 1.2 to 0.10 mol dm^{-3} in the photochemical reaction of AcrH^+ with diphenylmethane, comparable amounts of AcrH_2 and AcrHCHPh_2 are obtained in the ratio of 59 : 41.⁵⁴



The drastic change of the products in the presence of HClO_4 can be well explained by the reaction mechanism shown in Scheme 13. The reactions in both the absence and the presence of HClO_4 are initiated by photoinduced electron transfer from the alkylbenzene to the singlet excited state ($^1\text{AcrH}^{+*}$) to give the alkylbenzene radical cation–acridinyl radical pair. Since alkylbenzene radical cations are known as extremely strong carbon acids in solution,⁵⁵ they undergo proton loss from an α -carbon to yield the benzyl radical and analogs (R^\bullet).^{56,57} The deuterium isotope effects on the deprotonation processes are determined as 3.7 and 2.5 for toluene and ethylbenzene radical cations, respectively.⁵⁴ In the absence of HClO_4 , the two radical species (AcrH^\bullet and R^\bullet) are coupled efficiently to yield the adduct (AcrHR) selectively. The formation of AcrH^\bullet is detected by laser flash irradiation (355 nm from a Nd:YAG laser) of AcrH^+ in deaerated acetonitrile solution containing diphenylmethane as shown in Fig. 9, where transient absorption of AcrH^\bullet (a broad absorption band between 450 and 540 nm)⁵⁸ is observed clearly.⁵⁴ On the other hand, AcrH^\bullet can be proton-



Scheme 13.

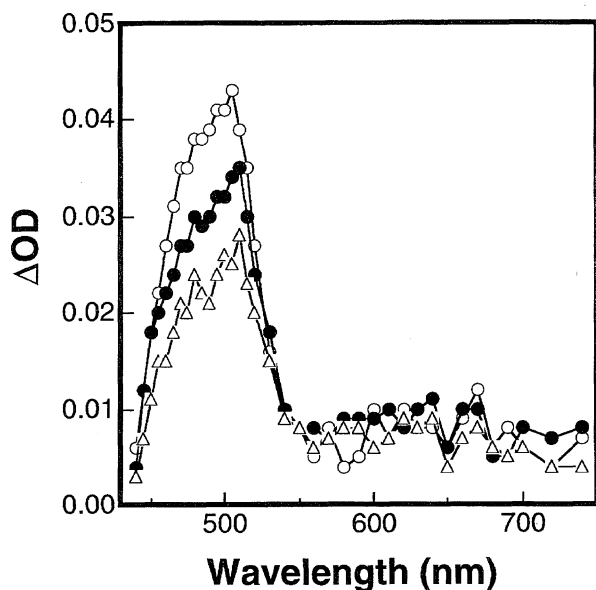


Fig. 9. The transient absorption spectra observed in laser flash photolysis of AcrH^\bullet ($5 \times 10^{-5} \text{ mol dm}^{-3}$) in deaerated acetonitrile containing diphenylmethane ($5 \times 10^{-2} \text{ mol dm}^{-3}$). Spectra were recorded 1 μs (\circ), 7 μs (\bullet), and 17 μs (\triangle) after the laser pulse.

ated in the presence of a large concentration of HClO_4 to give $\text{AcrH}_2^{\bullet+}$.²⁷⁾ Since the one-electron oxidation potentials of benzyl radical and analogs ($E_{\text{ox}}^0 = 0.73, 0.37, 0.16$, and 0.35 V vs. SCE for PhCH_2^\bullet , PhCHMe^\bullet , PhCMe_2^\bullet , and $\text{Ph}_2\text{CH}^\bullet$, respectively)⁵⁹⁾ are more negative than the reduction potential of $\text{AcrH}_2^{\bullet+}$ ($E_{\text{red}}^0 = 0.81 \text{ V}$),²⁷⁾ the electron transfer from R^\bullet to $\text{AcrH}_2^{\bullet+}$ is highly exergonic and thereby it proceeds efficiently to yield AcrH_2 and R^+ . The benzyl radical cation and analogs (R^+) undergo the nucleophilic addition of H_2O to yield benzyl alcohol derivatives (ROH). Thus, acid catalysis on electron transfer from R^\bullet to AcrH^\bullet plays an essential role to alter the products in the presence of HClO_4 (Scheme 13), although it does not affect the overall efficiency of the photochemical reaction significantly.

Catalysis of Metal Ions on Thermal Electron Transfer.

Acid catalysis on electron transfer can also be applied to catalysis of metal ions on electron transfer reactions, since not only protons but also metal ions are able to form strong bond with radical anions (Eqs. 1 and 2, where M corresponds to metal ions). It is certainly desired to detect such metal ion complexes of radical anions ($\text{A-M}^{\bullet-}$ and $\text{A-2M}^{\bullet-}$). We have recently succeeded in detecting the Mg^{2+} complexes of semiquinone radical anions.⁶⁰⁾

Although no electron transfer occurs from decamethylferrocene [$\text{Fe}(\text{Me}_5\text{C}_5)_2$] to p -benzoquinone (Q) in acetonitrile, the electron transfer is complete upon mixing [$\text{Fe}(\text{Me}_5\text{C}_5)_2$] and Q in the presence of $\text{Mg}(\text{ClO}_4)_2$. The transient electronic spectra of semiquinone radical anion in the presence of different concentrations of $\text{Mg}(\text{ClO}_4)_2$ are obtained by measuring the change in initial absorbance at various wavelengths with use of a stopped-flow spectrophotometer as shown in Fig. 10.⁶⁰⁾ The transient absorption spectrum of

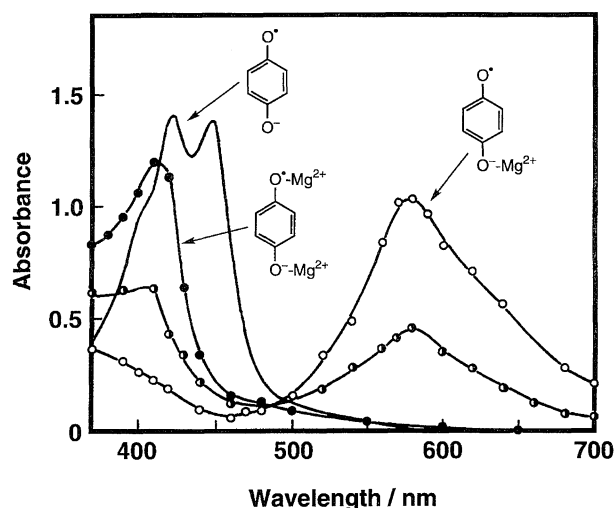
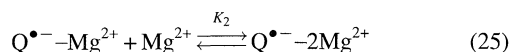
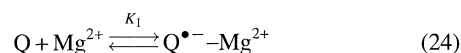


Fig. 10. Transient absorption spectra of semiquinone radical anion formed in electron transfer reduction of p -benzoquinone ($2.4 \times 10^{-4} \text{ mol dm}^{-3}$) by [$\text{Fe}(\text{Me}_5\text{C}_5)_2$] ($2.4 \times 10^{-3} \text{ mol dm}^{-3}$) in the presence of $\text{Mg}(\text{ClO}_4)_2$ [$1.0 \times 10^{-2} \text{ mol dm}^{-3}$ (\circ), $2.0 \times 10^{-1} \text{ mol dm}^{-3}$ (\bullet)] and by [$\text{Fe}(\text{MeC}_5\text{H}_4)_2$] ($2.4 \times 10^{-3} \text{ mol dm}^{-3}$) in the presence of $\text{Mg}(\text{ClO}_4)_2$ [1.6 mol dm^{-3} (\bullet)] in deaerated acetonitrile at 298 K. The solid line spectrum shows the absorption spectrum of semiquinone radical anion in the absence of $\text{Mg}(\text{ClO}_4)_2$, prepared by the reaction of p -benzoquinone ($2.4 \times 10^{-4} \text{ mol dm}^{-3}$) with $\text{Me}_4\text{N}^+\text{OH}^-$ ($2.4 \times 10^{-4} \text{ mol dm}^{-3}$) in deaerated acetonitrile at 298 K.

$\text{Q}^{\bullet-}$ in the presence of $1.0 \times 10^{-2} \text{ mol dm}^{-3} \text{ Mg}^{2+}$ ($\lambda_{\text{max}} = 590 \text{ nm}$) is significantly red-shifted as compared to that in the absence of Mg^{2+} ($\lambda_{\text{max}} = 422 \text{ nm}$).⁶¹⁾ Further addition of Mg^{2+} results in a blue shift to $\lambda_{\text{max}} = 415 \text{ nm}$ with a clean isosbestic point. Such spectroscopic changes indicate the formation of complexes between $\text{Q}^{\bullet-}$ and Mg^{2+} , which requires two steps. The first step is the formation of a 1 : 1 complex ($\text{Q}^{\bullet-}\text{-Mg}^{2+}$) and second step is an additional addition of Mg^{2+} to form a 1 : 2 complex ($\text{Q}^{\bullet-}\text{-2Mg}^{2+}$), as shown in Eqs. 24 and 25. Transient electronic spectra of the 1 : 1 and 1 : 2



complexes are also observed in the electron transfer reduction of 2,5-dichloro- p -benzoquinone and 2,5-dimethyl- p -benzoquinone. Although the formation constant K_1 for the 1 : 1 complex is too large to be determined, the formation constant K_2 for the 1 : 2 complex can be determined as listed in Table 2, where the K_2 value decreases with a decrease in the electron-donating ability of $\text{X-Q}^{\bullet-}$ ($\text{X} = 2,5\text{-Me}_2 > \text{H} > 2,5\text{-Cl}_2$). The formation of such complexes is also confirmed by the EPR spectra observed in the electron transfer reaction from $\text{Fe}(\text{MeC}_5\text{H}_4)_2$ to Q in the presence of Mg^{2+} in deaerated acetonitrile by applying a rapid-mixing EPR technique.⁶⁰⁾

No electron transfer from CoTPP (TPP =tetraphenylporphyrin dianion) to Q has occurred in acetonitrile at 298 K. In the presence of $\text{Mg}(\text{ClO}_4)_2$, however, efficient electron

Table 2. Absorption Maxima (λ_{\max}) of Semiquinone Radical Anions ($X-Q^{\bullet-}$), $X-Q^{\bullet-}-Mg^{2+}$, and $X-Q^{\bullet-}-2Mg^{2+}$ Complexes Formed in the Electron Transfer Reduction of $X-Q$ in the Presence of $Mg(ClO_4)_2$, and the Formation Constants of $X-Q^{\bullet-}-2Mg^{2+}$ (K_2) in the Electron Transfer Reduction of $X-Q$ and the Diels–Alder Reactions of 9,10-Dimethylantracene with $X-Q$ in Acetonitrile at 298 K

<i>p</i> -Benzoquinone form	λ_{\max}/nm			$K_2/dm^3 mol^{-1}$	
	$X-Q^{\bullet-}$	$X-Q^{\bullet-}-Mg^{2+}$	$X-Q^{\bullet-}-2Mg^{2+}$	a)	b)
<i>p</i> -Benzoquinone	422	590	410	4.5	3.9 (4.1) ^{c)}
2,5-Dichloro- <i>p</i> -benzoquinone	425	645	440	2.1	2.7
2,5-Dimethyl- <i>p</i> -benzoquinone	436	615	425	4.8	4.6

a) Determined from the spectral change in the presence of Mg^{2+} . b) Determined from the dependence of k_{obs} on $[Mg^{2+}]$ based on Eq. 27. The experimental errors are $\pm 10\%$. c) The value in parenthesis is obtained from an electron transfer from CoTPP to Q in the presence of Mg^{2+} in acetonitrile at 298 K. The experimental errors are $\pm 10\%$.

transfer from CoTPP to Q occurs to yield CoTPP⁺ (Eq. 26).⁶⁰ The electron transfer rates obeyed the second-order kinetics, showing a first-order dependence on each reactant concentration. The observed rate constant of electron transfer (k_{et}) increases with an increase in $[Mg^{2+}]$ to exhibit first-order dependence on $[Mg^{2+}]$ at low concentrations, changing to second-order dependence at high concentrations, as shown in Fig. 11a. Such dependence of k_{et} on $[Mg^{2+}]$ agrees well with that in Eq. 5 where **M** corresponds to Mg^{2+} . Equation 5 is rewritten as Eq. 27, the validity of which is confirmed by the linear plot of $(k_{et} - k_0)/[Mg^{2+}]$ vs. $[Mg^{2+}]$ for the data in Fig. 11. Thus, from the slope and intercept is obtained the K_2 value ($4.1 dm^3 mol^{-1}$), which agrees well with that ($4.5 dm^3 mol^{-1}$) determined directly from the spectral change of $Q^{\bullet-}$ in the presence of Mg^{2+} (Fig. 10).

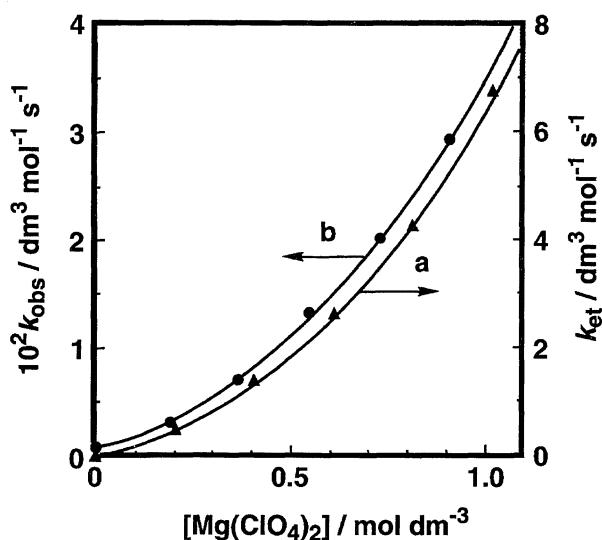
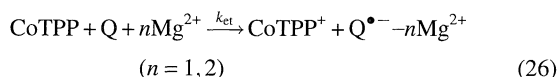
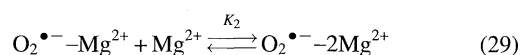
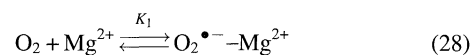


Fig. 11. Dependence of k_{et} and k_{obs} on $[Mg(ClO_4)_2]$ for (a) electron transfer from CoTPP ($1.0 \times 10^{-5} mol dm^{-3}$) to *p*-benzoquinone ($3.7 \times 10^{-3} mol dm^{-3}$) and (b) Diels–Alder reaction of 9,10-dimethylantracene ($1.3 \times 10^{-3} mol dm^{-3}$) with *p*-benzoquinone ($3.6 \times 10^{-2} mol dm^{-3}$) in the presence of $Mg(ClO_4)_2$ in deaerated acetonitrile at 298 K, respectively.

$$(k_{et} - k_0)/[Mg^{2+}] = k_0 K_1 (1 + K_2 [Mg^{2+}]), \quad (27)$$

Electron transfer from *cis*- $[R_2Co(bpy)_2]^+$ to Q also occurs efficiently in the presence of Mg^{2+} in acetonitrile, although no electron transfer occurs in the absence of Mg^{2+} .⁶² The observed rate constant of electron transfer (k_{et}) also exhibits first-order dependence on $[Mg^{2+}]$ at low concentrations, changing to second-order dependence at high concentrations.⁶² The rate of electron transfer is further increased by the presence of both $Mg(ClO_4)_2$ and $HClO_4$. Thus, the k_{et} value for electron transfer from *cis*- $[Et_2Co(bpy)_2]^+$ to Q in the presence of $Mg(ClO_4)_2$ ($1.0 mol dm^{-3}$) and $HClO_4$ ($0.10 mol dm^{-3}$) in acetonitrile at 298 K is $5.2 \times 10^2 dm^3 mol^{-1} s^{-1}$, which is 5.2×10^{16} times faster than the rate constant without $Mg(ClO_4)_2$ or $HClO_4$ ($1.0 \times 10^{-14} dm^3 mol^{-1} s^{-1}$) which is estimated from the correlation between $\log k_{et}$ vs. E_{red}^0 of the oxidants.⁶²

The Mg^{2+} is also effective for electron transfer reduction of O_2 in acetonitrile.⁶³ Thus, efficient electron transfer from $[Fe(Me_5C_5)_2]$ to O_2 occurs in the presence of Mg^{2+} in acetonitrile at 298 K to yield $[Fe(Me_5C_5)_2]^+$, although no electron transfer occurs from $[Fe(Me_5C_5)_2]$ to O_2 in the absence of Mg^{2+} under otherwise the same experimental conditions.⁶³ The observed pseudo-first-order rate constant of electron transfer (k_{et}) in an O_2 -saturated acetonitrile solution exhibits a similar dependence on $[Mg^{2+}]$ to that observed in the electron transfer reduction of Q as shown in Fig. 12a, i.e., first-order and second-order dependence on $[Mg^{2+}]$ at low and high Mg^{2+} concentrations, respectively. This indicates that $O_2^{\bullet-}$ forms complexes with Mg^{2+} with 1 : 1 and 1 : 2 stoichiometries at low and high Mg^{2+} concentrations (Eqs. 28 and 29), respectively. From the linear plot of $(k_{et} - k_0)/[Mg^{2+}]$ vs. $[Mg^{2+}]$ in Fig. 12b is obtained the K_2 value ($3.2 dm^3 mol^{-1}$) for the 1 : 2 complex between $O_2^{\bullet-}$ and Mg^{2+} .



In order to examine catalysis on electron transfer reduction of various oxidants, it is better to find an appropriate electron donor which undergoes the irreversible electron transfer oxidation. In this context we have recently reported that 10,10'-dimethyl-9,9',10,10'-tetrahydro-9,9'-biacridine

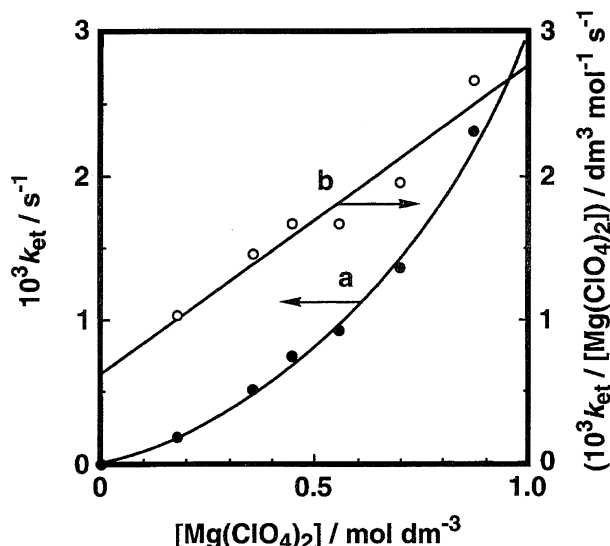
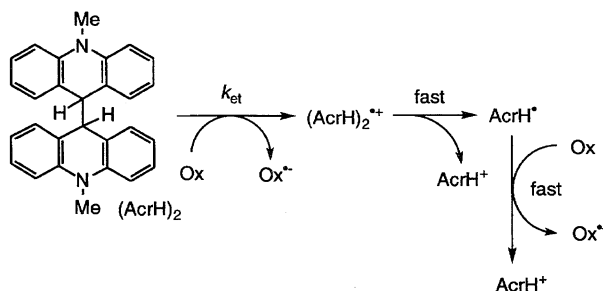


Fig. 12. Plots of (a) k_{et} vs. $[Mg(ClO_4)_2]$ and (b) $k_{et}/[Mg(ClO_4)_2]$ vs. $[Mg(ClO_4)_2]$ for electron transfer from $[Fe(Me_5C_5)_2]$ ($5.3 \times 10^{-4} \text{ mol dm}^{-3}$) to O_2 ($1.3 \times 10^{-2} \text{ mol dm}^{-3}$) in the presence of $Mg(ClO_4)_2$ in O_2 -saturated acetonitrile at 298 K.

$[(AcrH)_2]$, prepared by the one-electron reduction of $AcrH^+$ by $Me_3SnSnMe_3$,⁶⁴ acts as a two-electron donor accompanied by the cleavage of the C(9)–C bond instead of the C(9)–H bond in the outer-sphere electron transfer reactions with various inorganic and organic oxidants.^{65,66} The initial electron transfer from $(AcrH)_2$ to oxidants (Ox) is the rate-determining step, followed by facile cleavage of the C(9)–C bond of $(AcrH)_2^{\bullet+}$ to yield $AcrH^+$ and $AcrH^{\bullet}$ as shown in Scheme 14. The second electron transfer from $AcrH^{\bullet}$ to Ox is much faster than the initial electron transfer, since the one-electron oxidation potential of $AcrH^{\bullet}$ is largely negative ($E_{ox}^0 = -0.43 \text{ V}$)¹⁶) as compared with that of $(AcrH)_2$ ($E_{ox}^0 = 0.62 \text{ V}$).⁶⁶ Thus, even if initial electron transfer is endergonic ($\Delta G_{et}^0 > 0$), the electron transfer reduction of Ox proceeds efficiently provided that the E_{red}^0 values of oxidants are more positive than -0.43 V . Thus, the plot of $\log k_{et}$ vs. E_{red}^0 in Fig. 13 demonstrates a typical dependence of the rate constant (k_{et}) for outer-sphere electron transfer reactions; the $\log k_{et}$ value increases linearly with an increase in the E_{red}^0 value with a slope of $F/(2.3RT)$ ($=16.9$ at 298 K) to reach a diffusion-limited value ($k_{et} = 2.0 \times 10^{10} \text{ dm}^3 \text{ mol}^{-1} \text{ s}^{-1}$).⁶⁶ It should be noted that the rate constant is solely determined



Scheme 14.

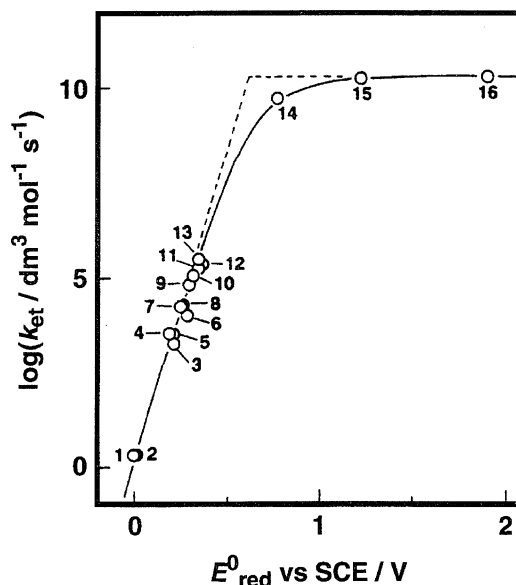
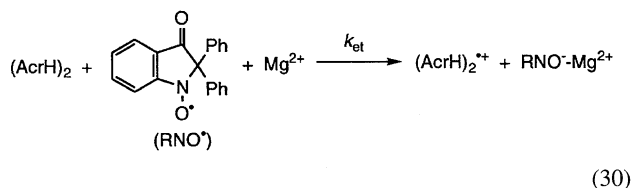


Fig. 13. Plot of $\log k_{et}$ vs. E_{red}^0 for the electron transfer reactions from $(AcrH)_2$ to one-electron oxidants in acetonitrile at 298 K. The numbers refer to oxidants (1: bromanil, 2: chloranil, 3: Ph_3C^+ , 4: TCNQ, 5: TCNE, 6: 2,3-dicyano-*p*-benzoquinone, 7: $[Fe(Bu_5H_4)_2]^+$, 8: $[Fe(Me_5C_5H_4)_2]^+$, 9: $[Fe(C_5H_5)(Bu_5C_5H_4)]^+$, 10: $Fe(C_5H_5)(t\text{-}amylC_5H_4)^+$, 11: CoTPP, 12: $Fe(C_5H_5)_2^+$, 13: $[Fe(C_5H_5)(HgClC_5H_4)]^+$, 14: $[Ru(bpy)_3]^{2+*}$, 15: pyrene*, 16: 9,10-dicyanoanthracene*).

by the E_{red}^0 value, and is insensitive to the size of oxidants. Thus, the dimer $[(AcrH)_2]$ acts as not only a unique two-electron donor without release of a proton but also a novel outer-sphere organic electron donor.

Although no electron transfer occurs from $(AcrH)_2$ to 2,3-dihydro-3-oxo-2,2-diphenyl-1*H*-indol-1-ylxyl radical (RNO $^{\bullet}$) in acetonitrile at 298 K, consistent with the largely negative reduction potential of the radical ($E_{red}^0 = -0.87 \text{ V}$), the electron transfer occurs efficiently in the presence of $Mg(ClO_4)_2$ as shown in Eq. 30.⁶⁷ The k_{et} value increases linearly with an increase in $[Mg^{2+}]$ as shown in Fig. 14a, indicating the 1 : 1 complex formation between the resulting RNO^- anion and Mg^{2+} , since no interaction between Mg^{2+} and the RNO^{\bullet} radical has been detected in the electronic spectra in the presence of Mg^{2+} . Similarly electron transfer from $(AcrH)_2$ to 1,1-diphenyl-2-picrylhydrazyl (DPPH $^{\bullet}$) occurs efficiently (Eq. 31), and the k_{et} value also increases linearly with an increase in $[Mg^{2+}]$ as shown in Fig. 15a.⁶⁷



Mechanistic Insight of Catalysis of Metal Ions on Electron Transfer into Diels–Alder Reaction. If catalysis

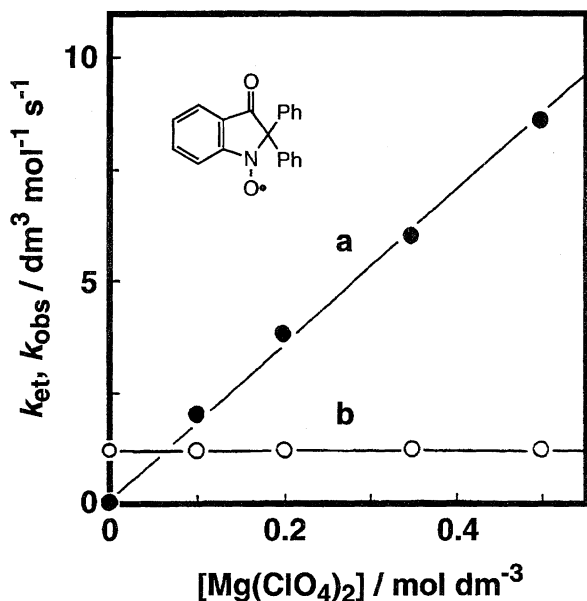


Fig. 14. Dependence of k_{et} and k_{obs} on $[\text{Mg}(\text{ClO}_4)_2]$ for (a) electron transfer from $(\text{AcrH})_2$ to RNO^\bullet and (b) hydrogen transfer from AcrH_2 to RNO^\bullet in the presence of $\text{Mg}(\text{ClO}_4)_2$ in deaerated acetonitrile at 323 K, respectively.

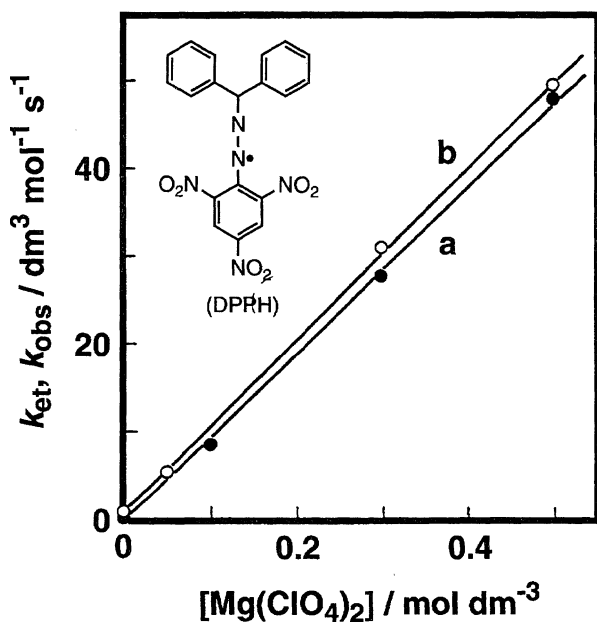


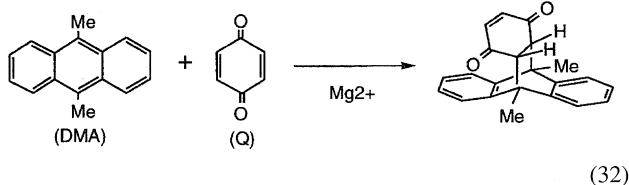
Fig. 15. Dependence of k_{et} and k_{obs} on $[\text{Mg}(\text{ClO}_4)_2]$ for (a) electron transfer from $(\text{AcrH})_2$ to DPPH^\bullet in deaerated acetonitrile at 313 K and (b) hydrogen transfer from AcrH_2 to DPPH^\bullet in the presence of $\text{Mg}(\text{ClO}_4)_2$ in deaerated acetonitrile at 298 K, respectively.

of metal ions on electron transfer plays an essential role in some reactions, formulated previously as ionic or concerted reactions, the dependence of the rate constants on the metal ion concentration would be the same as that observed in the electron transfer reduction of the same substrate. Thus, the comparison of the catalytic function of metal ions in electron transfer reactions with that in apparently polar or concerted

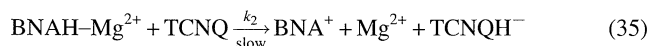
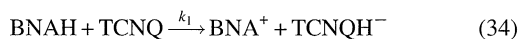
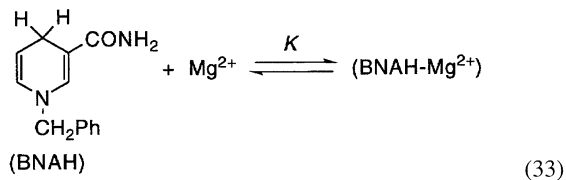
reactions of the same substrate would provide valuable insight into the mechanistic viability of electron transfer.

Diels–Alder reactions are usually regarded as concerted processes where the interaction between HOMOs of dienes and LUMOs of dienophiles determines the reactivity.⁶⁸⁾ When electron-rich dienes having high-lying HOMOs react with electron-deficient dienophiles having low-lying LUMOs, however, electron transfer from the diene to the dienophile plays an important role as the activation step.^{69,70)} The interaction of metal ions with radical anions of dienophiles may enhance the electron affinity of the dienophiles so that electron transfer may provide a favorable reaction pathway for such dienophiles. In fact, the [4+2] cycloaddition of 9,10-dimethylantracene (DMA) with *p*-benzoquinone (Q) occurs efficiently in the presence of $\text{Mg}(\text{ClO}_4)_2$ ($9.09 \times 10^{-1} \text{ mol dm}^{-3}$) to yield the adduct selectively (Eq. 32),⁶⁰⁾ although *p*-benzoquinone derivatives have been regarded as inert or weak dienophiles.⁷¹⁾ The [4+2] cycloaddition of anthracene and 9-methylantracene with other *p*-benzoquinone derivatives (X-Q ; $\text{X} = 2,5\text{-Cl}_2$ and $2,5\text{-Me}_2$) also occurs efficiently in the presence of $\text{Mg}(\text{ClO}_4)_2$ to yield the corresponding adducts.⁶⁰⁾ The observed second-order rate constant (k_{obs}) increases with an increase in $[\text{Mg}^{2+}]$ to exhibit first-order dependence on $[\text{Mg}^{2+}]$ at low concentrations, changing to second-order dependence at high concentrations, as shown in Fig. 11b.⁶⁰⁾ There is a striking similarity with respect to the dependence of k_{obs} on $[\text{Mg}^{2+}]$ between the electron transfer reaction (Fig. 11a) and the Diels–Alder reaction (Fig. 11b), despite the large difference in their reactivities. Thus, the same plot as employed for the Mg^{2+} -catalyzed electron transfer (Eq. 27) also gives a straight line for the Diels–Alder reaction of DMA with Q. The K_2 values obtained from the linear plots for the Diels–Alder reaction of DMA with X-Q in acetonitrile at 298 K are also listed in Table 2, where the K_2 values agree well with those obtained directly from the spectral change of $\text{X-Q}^{\bullet-}$ in the presence of Mg^{2+} as well as those determined from the electron transfer reactions. Such agreements for each quinone strongly suggest that the catalysis of Mg^{2+} in the Diels–Alder reactions of DMA with X-Q is essentially the same as that in the electron transfer reduction of X-Q . Thus, the Mg^{2+} -catalyzed electron transfer from anthracenes to X-Q may be a rate-determining step of the Diels–Alder reactions. In such a case, the K_2 values should be the same, irrespective of anthracene derivatives, since the formation of 1 : 2 complex of $\text{Q}^{\bullet-}$ and Mg^{2+} is independent of anthracene derivatives. In fact, the K_2 values derived from the Diels–Alder reactions of DMA, 9-methylantracene, and anthracene with Q in acetonitrile at 333 K are the same ($K_2 = 2.1 \pm 0.3 \text{ dm}^3 \text{ mol}^{-1}$), despite the significant difference in their reactivities; $k_0K_1 = 3.5 \times 10^{-2}$, 6.2×10^{-3} , and $1.4 \times 10^{-4} \text{ dm}^6 \text{ mol}^{-2} \text{ s}^{-1}$, respectively.⁶⁰⁾ Moreover, it has been confirmed that no 1 : 2 complex is formed between Q and Mg^{2+} .⁶⁰⁾ Thus, the role of Mg^{2+} to activate the weak dienophiles (X-Q) is ascribed to the 1 : 1 and 1 : 2 complex formation of $\text{X-Q}^{\bullet-}$ and Mg^{2+} , which results in an increase in the rate of electron transfer from anthracenes as well as one-electron reductants to X-Q with an increase in $[\text{Mg}^{2+}]$, ex-

hibiting first-order and second-order dependence on $[\text{Mg}^{2+}]$, respectively.



Mechanistic Insight of Catalysis of Metal Ions on Electron Transfer into Hydride Transfer Reactions. The effects of metal ions such as Mg^{2+} and Zn^{2+} ions on hydride transfer reactions from NADH model compounds to substrates have attracted considerable interest in relation to the role of metal ions in the redox reactions of nicotinamide coenzymes.⁷²⁾ The effects of Mg^{2+} on hydride transfer reactions from a typical NADH model compound, 1-benzyl-1,4-dihydronicotinamide (BNAH), to substrates are rather complex. When a relatively strong oxidant such as 7,7,8,8-tetracyano-*p*-quinodimethane (TCNQ) is employed as a substrate, the addition of Mg^{2+} to the BNAH–TCNQ system in anhydrous acetonitrile causes a significant decrease in the reaction rate.¹³⁾ The rate constant of hydride transfer from BNAH to TCNQ decreases with an increase in $[\text{Mg}^{2+}]$ to reach a constant value which is 23 times smaller than that in the absence of Mg^{2+} ($1.64 \times 10^3 \text{ dm}^3 \text{ mol}^{-1} \text{ s}^{-1}$). Such a retarding effect of Mg^{2+} is well interpreted by the 1 : 1 complex formation between BNAH and Mg^{2+} (Eq. 33), which reacts with TCNQ at a much slower rate than BNAH (Eqs. 34 and 35).



In such a case, the dependence of the observed second-order rate constant k_{obs} on $[\text{Mg}^{2+}]$ is given by Eq. 36, where k_1 and k_2 are the rate constants of free BNAH (Eq. 34) and the Mg^{2+} complex (Eq. 35), respectively. The K value for the complex formation between BNAH and Mg^{2+} is determined as $1.1 \times 10^4 \text{ dm}^3 \text{ mol}^{-1}$ from the dependence of k_{obs} on $[\text{Mg}^{2+}]$ (Eq. 36), agreeing well with that determined by the spectroscopic change of BNAH due to the complex formation with Mg^{2+} ($1.2 \times 10^4 \text{ dm}^3 \text{ mol}^{-1}$).⁷³⁾ Since there is no interaction between $\text{TCNQ}^{\bullet-}$ and Mg^{2+} , the reduction potential of TCNQ is not affected by the presence of Mg^{2+} .⁷³⁾ On the other hand, the one-electron oxidation potentials of BNAH (0.57 V vs. SCE) in acetonitrile is significantly shifted to the positive direction by the complexation with Mg^{2+} (0.80 V vs. SCE).⁷⁴⁾ Thus, the significant decrease in the reactivity of BNAH by the complexation with Mg^{2+} is consistent with the decrease in the electron donor ability.

$$k_{\text{obs}} = (k_1 + k_2 K [\text{Mg}^{2+}]) / (1 + K [\text{Mg}^{2+}]) \quad (36)$$

When TCNQ is replaced by a weaker oxidant such as 2,6-dichloro-*p*-benzoquinone, the Mg^{2+} ion shows both retarding and accelerating effects on the hydride transfer reaction depending on the Mg^{2+} concentration, as shown in Fig. 16, where the observed second-order rate constant (k_{obs}) decreases sharply from the value in the absence of Mg^{2+} ($7.5 \times 10 \text{ dm}^3 \text{ mol}^{-1} \text{ s}^{-1}$) with an increase in $[\text{Mg}^{2+}]$ at low concentrations ($\ll 0.10 \text{ mol dm}^{-3}$), while the k_{obs} value increases at the higher concentrations ($> \text{ca. } 0.10 \text{ mol dm}^{-3}$).⁷⁴⁾ The change of the E_{red}^0 values of *p*-benzoquinone derivatives in the presence of various concentrations of Mg^{2+} was determined by the analysis of the cyclic voltammograms at various sweep rates.⁷⁴⁾ The sharp decrease in the rate constant from the value in the absence of Mg^{2+} to that in the presence of Mg^{2+} (0.10 mol dm^{-3}) can be well understood, since the positive shift of the E_{ox}^0 value (+0.23 V) of BNAH from the value in the absence of Mg^{2+} to that in the presence of Mg^{2+} (0.10 mol dm^{-3}) is larger than the corresponding positive shift of the E_{red}^0 value of 2,6-dichloro-*p*-benzoquinone (0.14 V). In the presence of a large concentration of Mg^{2+} (1.6 mol dm^{-3}), however, the positive shift of the E_{red}^0 value of the quinone (+0.21 V) becomes comparable with the corresponding positive shift of BNAH (+0.18 V), agreeing with the recovery of the reactivity at the high Mg^{2+} concentration as compared to that in the absence of Mg^{2+} (Fig. 16).⁷⁴⁾ Thus, the change of the k_{obs} values depending on $[\text{Mg}^{2+}]$ is caused by the corresponding change in the free energy change of electron transfer from BNAH to the substrate in the presence of Mg^{2+} , $\Delta G_{\text{et}}^{0*}$, which is given by $F(E_{\text{ox}}^{0*} - E_{\text{red}}^{0*})$, where $*$ denotes the value in the presence of Mg^{2+} . Such a dependence of k_{obs} on $\Delta G_{\text{et}}^{0*}$ is generally shown for various *p*-benzoquinone derivatives at different Mg^{2+} concentrations (vide infra).

The log k_{obs} value for the hydride transfer from BNAH to

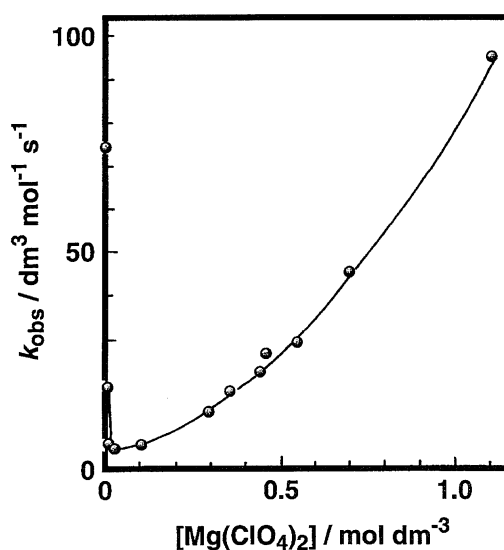


Fig. 16. Plot of k_{obs} vs. $[\text{Mg}(\text{ClO}_4)_2]$ for the hydride transfer reaction from BNAH to 2,6-dichloro-*p*-benzoquinone in the presence of $\text{Mg}(\text{ClO}_4)_2$ in acetonitrile at 298 K.

various *p*-benzoquinones in the absence of Mg^{2+} shows a smooth but somehow curved correlation with the $E_{\text{ox}}^0 - E_{\text{red}}^0$ value as shown by open circles in Fig. 17.⁷⁴⁾ On the other hand, the addition of Mg^{2+} (0.10 mol dm^{-3}) to the BNAH-Q system results in both the increase and decrease of the $\log k_{\text{obs}}$ values for *p*-benzoquinone derivatives having lower reduction potentials ($E_{\text{red}}^0 < -0.18 \text{ V}$) and higher reduction potentials ($E_{\text{red}}^0 > 0 \text{ V}$), respectively. The accelerating effect of Mg^{2+} is enhanced by increasing the Mg^{2+} concentration from 0.10 to 1.6 mol dm^{-3} , while the retarding effect of Mg^{2+} is unchanged by increasing the Mg^{2+} concentration (Fig. 17). When the $\log k_{\text{obs}}$ values in the presence of Mg^{2+} in Fig. 17 are replotted against the difference between the one-electron redox potentials of BNAH and Q in the presence of Mg^{2+} , $E_{\text{ox}}^{0*} - E_{\text{red}}^{0*}$, the three different correlation observed in Fig. 17 emerge as a single and unified one, as shown in Fig. 18.⁷⁴⁾ Such a remarkable transformation of the plots in Fig. 17 to the single and unified correlation in Fig. 18 demonstrates clearly that the retarding and accelerating effects of Mg^{2+} on the rate constants of the hydride transfer reactions are directly related to the change of the one-electron redox potentials of BNAH and Q in the presence of Mg^{2+} . This indicates that electron transfer from BNAH to Q is the rate-determining step which determines the overall reactivity of the hydride transfer reactions in the absence and presence of

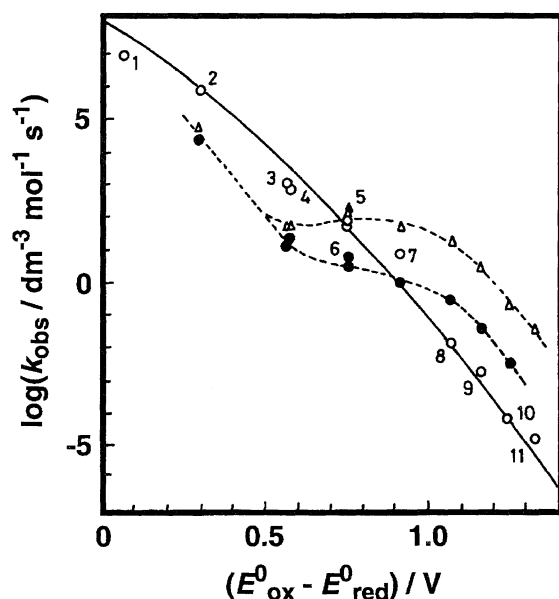


Fig. 17. Plots of k_{obs} for the hydride transfer reactions from BNAH to *p*-benzoquinone derivatives in the absence (○) and presence of 0.10 mol dm⁻³ (●) and 1.6 mol dm⁻³ (△) Mg²⁺ ion vs. the difference of the one-electron redox potentials between BNAH and *p*-benzoquinone derivatives in the absence of Mg²⁺ ion in acetonitrile, $E_{\text{ox}}^0 - E_{\text{red}}^0$. Numbers refer to *p*-benzoquinone derivatives (1: 2,3-dichloro-5,6-dicyano-*p*-benzoquinone, 2: 2,3-dicyano-*p*-benzoquinone, 3: chloranil, 4: bromanil, 5: 2,6-dichloro-*p*-benzoquinone, 6: 2,5-dichloro-*p*-benzoquinone, 7: chloro-*p*-benzoquinone, 8: *p*-benzoquinone, 9: methyl-*p*-benzoquinone, 10: 2,6-dimethyl-*p*-benzoquinone, 11: trimethyl-*p*-benzoquinone).

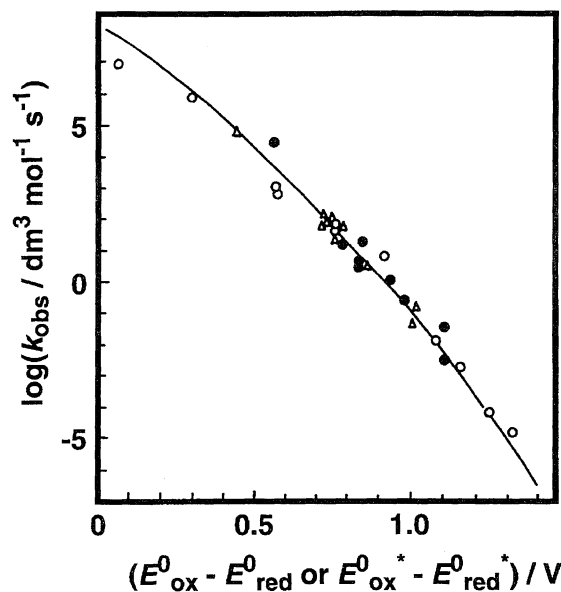
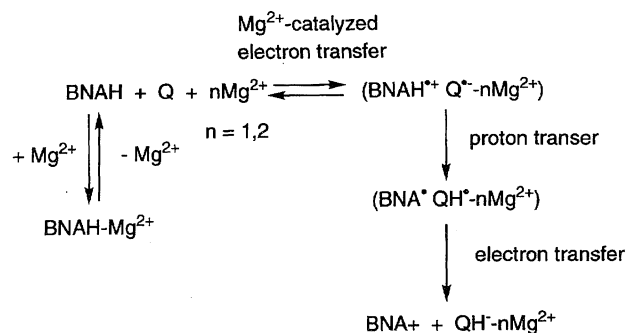


Fig. 18. Plot of $\log k_{\text{obs}}$ for the hydride transfer reactions from BNAH to *p*-benzoquinone derivatives in the absence (○) and presence of 0.10 mol dm⁻³ (●) and 1.6 mol dm⁻³ (△) Mg²⁺ ion vs. the difference of the one-electron redox potentials between BNAH and *p*-benzoquinone derivatives in the absence ($E_{\text{ox}}^0 - E_{\text{red}}^0$) and presence of 0.10 and 1.6 mol dm⁻³ Mg²⁺ ion ($E_{\text{ox}}^0 * - E_{\text{red}}^0 *$), respectively. The numbers refer to *p*-benzoquinone derivatives in Fig. 17.

Mg^{2+} , as shown in Scheme 15.⁷⁴⁾ The electron transfer from BNAH to Q is accelerated by the complexation of Mg^{2+} with $\text{Q}^{\bullet-}$, while the complexation of Mg^{2+} with BNAH retards the electron transfer. With an increase in the Mg^{2+} concentration, not only one Mg^{2+} but also two Mg^{2+} ions can form the complex with $\text{Q}^{\bullet-}$, resulting in a second-order dependence of k_{obs} with respect to $[\text{Mg}^{2+}]$, as shown in Fig. 16. The electron transfer may be followed by the proton transfer from $\text{BNAH}^{\bullet+}$ to the Mg^{2+} complex of $\text{Q}^{\bullet-}$, and the subsequent electron transfer from BNA^{\bullet} to the Mg^{2+} complex of QH^{\bullet} may occur efficiently, judging from the largely negative oxidation potential of BNA^{\bullet} (-1.1 V vs. SCE).¹⁶⁾ The observed primary kinetic isotope effects $k_{\text{H}}/k_{\text{D}}$ are well analyzed as those on the proton transfer process.⁷⁴⁾

Hydride reduction of oxygen by 1,5-dihydroflavin-2',3',4',5'-tetraacetate anion (FIH^-) is also catalyzed by the presence of Mg^{2+} in acetonitrile.⁽⁶³⁾ The reduction of oxygen by



Scheme 15.

the 1,5-dihydroflavin anion is known to be a key step in biological oxidation involving flavoproteins.⁷⁵⁾ An electron transfer mechanism has often been proposed for the reaction of 1,5-dihydroflavin with oxygen, since direct one-step reaction to give a covalent bond is spin-forbidden.^{76,77)} However, the facile follow-up reaction to give the covalent flavin-4a-hydroperoxide following the possible electron transfer has precluded the direct detection of the radical ion pair.⁷⁶⁾ In such a case, the comparison of the catalytic effects of Mg^{2+} on the hydride transfer reaction with that of electron transfer reduction of oxygen provides valuable insight into the viability of the electron transfer mechanism.

The observed pseudo-first-order rate constant (k_{obs}) of the Mg^{2+} -catalyzed hydride transfer from FIH^- to O_2 increases linearly with an increase in $[\text{Mg}(\text{ClO}_4)_2]$, as shown in Fig. 19.⁶³⁾ Although the dependence of k_{obs} on $[\text{Mg}^{2+}]$ in

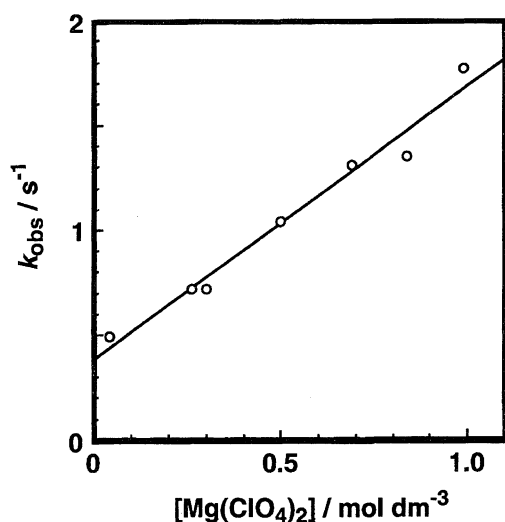
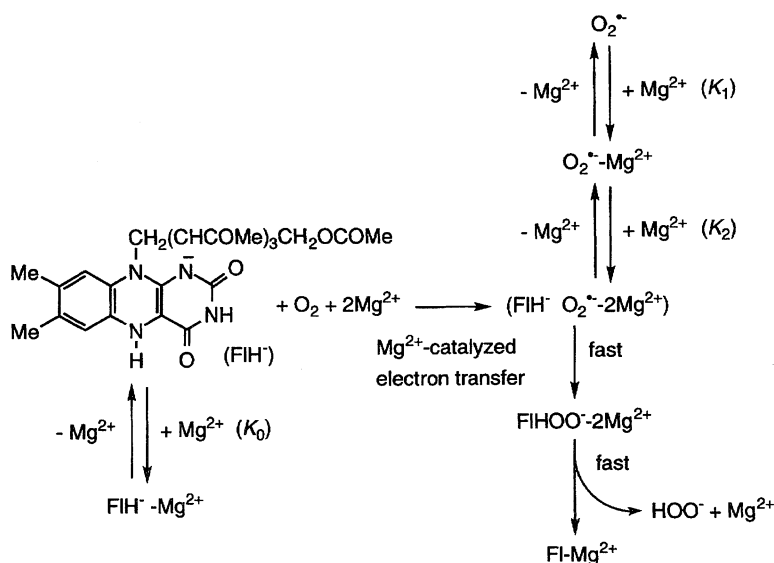


Fig. 19. Plot of k_{obs} vs. $[\text{Mg}(\text{ClO}_4)_2]$ for reduction of O_2 ($1.3 \times 10^{-3} \text{ mol dm}^{-3}$) by FIH^- ($1.2 \times 10^{-4} \text{ mol dm}^{-3}$) in the presence of $\text{Mg}(\text{ClO}_4)_2$ in acetonitrile at 298 K.

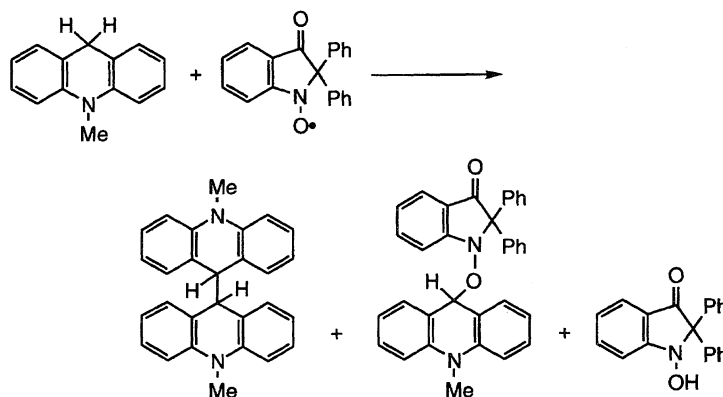
Fig. 19 is apparently different from that for the Mg^{2+} -catalyzed electron transfer reduction of oxygen in Fig. 12a, the difference can be well interpreted by the complex formation between FIH^- and Mg^{2+} (vide infra). Flavins themselves are known to form complexes with Mg^{2+} in acetonitrile.⁷⁸⁾ The reduced flavin anion FIH^- has also been reported to form the complex with Mg^{2+} .⁷⁹⁾ Since the Mg^{2+} complex of FIH^- is a much weaker one-electron donor than free FIH^- , free FIH^- which is in equilibrium with $\text{FIH}^- \text{--} \text{Mg}^{2+}$ may be involved in the Mg^{2+} -catalyzed electron transfer to O_2 to give radical pair ($\text{FIH}^\bullet \text{O}_2^{\bullet-} \text{--} 2\text{Mg}^{2+}$). Since the spin density of FIH^\bullet is greater at the C-4a position (0.30) than those at the other carbons, the radical coupling between FIH^\bullet and $\text{O}_2^{\bullet-} \text{--} 2\text{Mg}^{2+}$ may occur selectively at the C-4a position to give flavin 4a-hydroperoxide which decomposes to FI and hydrogen peroxide, as shown in Scheme 16.⁶³⁾ If one assumes that the Mg^{2+} -catalyzed electron transfer from FIH^- to O_2 is the rate determining step, the dependence of k_{obs} on $[\text{Mg}^{2+}]$ is given by Eq. 37, where k'_0 is the rate constant in the absence of Mg^{2+} , K_0 is the formation constant of $\text{FIH}^- \text{--} \text{Mg}^{2+}$, K_1 and K_2 are the formation constants of $\text{O}_2^{\bullet-} \text{--} \text{Mg}^{2+}$ and $\text{O}_2^{\bullet-} \text{--} 2\text{Mg}^{2+}$, respectively ($K_1[\text{Mg}^{2+}] \gg 1$). In fact, the dependence of k_{obs} on $[\text{Mg}^{2+}]$ in Fig. 19 is the same as expected from Eq. 37. Moreover, the K_2 value is derived from the intercept and slope of Fig. 19 as $3.4 \pm 0.3 \text{ dm}^3 \text{ mol}^{-1}$, which agrees well with the K_2 value ($3.2 \pm 0.3 \text{ dm}^3 \text{ mol}^{-1}$) obtained independently from Mg^{2+} -catalyzed electron transfer in Fig. 12b. Such agreement strongly indicates that Mg^{2+} -catalyzed electron transfer from FIH^- to O_2 is the rate-determining step for reduction of O_2 with FIH^- in the presence of Mg^{2+} (Scheme 16).

$$k_{\text{obs}} = k'_0 K_1 (1 + K_2 [\text{Mg}^{2+}]) / K_0 \quad (37)$$

Mechanistic Insight of Catalysis of Metal Ions on Electron Transfer into Hydrogen Transfer Reactions. There are two possibilities in the mechanisms of hydrogen transfer reactions, i.e., a one-step hydrogen transfer or electron transfer followed by proton transfer.⁸⁰⁾ The catalytic effects



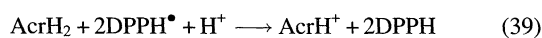
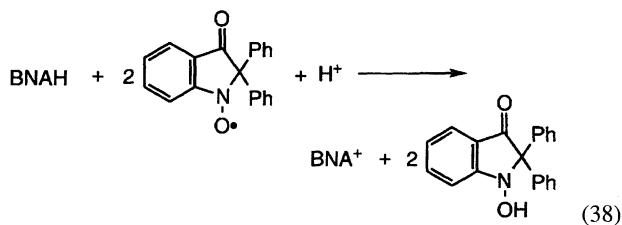
Scheme 16.



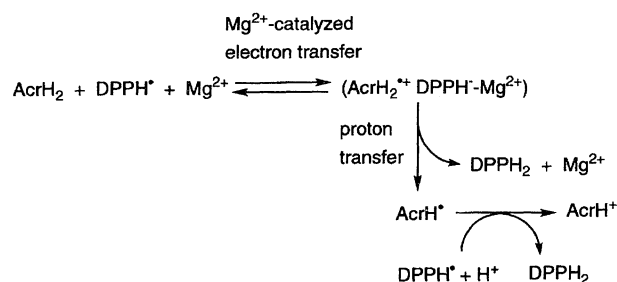
Scheme 17.

of metal ions provide a reliable criterion for distinguishing between the one-step hydrogen transfer and electron transfer mechanisms.

The RNO^\bullet radical employed for the Mg^{2+} -catalyzed electron transfer reduction by $(\text{AcrH})_2$ is stable in acetonitrile. When AcrH_2 was added to an acetonitrile solution of the RNO^\bullet radical, hydrogen transfer from AcrH_2 to the RNO^\bullet radical occurs to yield the dimer, the adduct, and the corresponding 1-hydroxy compound as shown in Scheme 17.⁶⁷⁾ When AcrH_2 was replaced by BNAH , however, no adduct was formed when BNAH was oxidized to BNA^+ . The stoichiometry of the reaction of BNAH with RNO^\bullet is given by Eq. 38.⁶⁷⁾ Such difference in the stoichiometry between AcrH_2 and BNAH may be ascribed to the difference in the electron-donor ability of AcrH^\bullet and BNA^\bullet . The electron transfer from AcrH^\bullet to the RNO^\bullet radical is endergonic judging from the one-electron oxidation potential of AcrH^\bullet (E_{ox}^0 vs. $\text{SCE} = -0.43 \text{ V}$)¹⁶⁾ and the one-electron reduction potential of the RNO^\bullet radicals ($E_{\text{red}}^0 = -0.66$ and -0.87 for **1** and **2**, respectively).⁶⁷⁾ In contrast, electron transfer from BNA^\bullet (E_{ox}^0 vs. $\text{SCE} = -1.08 \text{ V}$)¹⁶⁾ to the RNO^\bullet radicals is exergonic. Thus, electron transfer from BNA^\bullet to the RNO^\bullet radicals occurs following hydrogen transfer from BNAH to yield BNA^+ and the corresponding 1-hydroxy compound, leading to the overall stoichiometry in Eq. 38. The same stoichiometry is found for the reaction of AcrH_2 with 1,1-diphenyl-2-picrylhydrazyl (DPPH^\bullet) as shown in Eq. 39, since electron transfer from AcrH^\bullet ($E_{\text{ox}}^0 = -0.43 \text{ V}$)¹⁶⁾ to DPPH^\bullet ($E_{\text{red}}^0 = 0.24 \text{ V}$) is also energetically feasible.⁶⁷⁾



If the hydrogen transfer from AcrH_2 to the radicals involves an electron-transfer process as the rate-determining step, the rate of hydrogen transfer would also be accelerated by the presence of Mg^{2+} , as observed for electron transfer re-



Scheme 18.

actions from $(\text{AcrH})_2$ to the radicals (Figs. 14a and 15a). The effect of Mg^{2+} on the rates of hydrogen transfer from AcrH_2 to the RNO^\bullet radical is also shown in Fig. 14b, where no effect of Mg^{2+} on the k_{obs} values is observed, demonstrating a sharp contrast with the case of the electron-transfer reaction from $(\text{AcrH})_2$ to the RNO^\bullet radical (Fig. 14a).⁶⁷⁾ Thus, there may be no contribution of electron transfer from AcrH_2 to the RNO^\bullet radical in the hydrogen-transfer reaction, which may thereby proceed via a one-step hydrogen-transfer process. In fact a large primary kinetic isotope effect was observed ($k_{\text{H}}/k_{\text{D}} = 21$ at 323 K) when AcrH_2 is replaced by the 9,9-dideuterated analogue (AcrD_2).⁶⁷⁾ On the other hand, electron transfer from $(\text{AcrH})_2$ to DPPH^\bullet is also catalyzed by the presence of Mg^{2+} , as shown in Fig. 15a. In contrast with the case of the RNO^\bullet radical, Mg^{2+} also accelerates significantly the rate of hydrogen transfer from AcrH_2 to DPPH^\bullet , as shown in Fig. 15b.⁶⁷⁾ Thus, the hydrogen transfer may proceed via electron transfer from AcrH_2 to DPPH^\bullet , which is accelerated by the presence of Mg^{2+} , followed by proton transfer from $\text{AcrH}_2^{\bullet+}$ to DPPH^- to yield DPPH_2 (Scheme 18).⁶⁷⁾ The resulting acridinyl radical (AcrH^\bullet) is a much stronger reductant than AcrH_2 , judging from the more negative oxidation potential (-0.43 V)¹⁶⁾ than that of AcrH_2 (0.81 V),²⁷⁾ and thereby AcrH^\bullet can readily transfer an electron to another DPPH^\bullet molecule to yield AcrH^+ (Scheme 18). The primary kinetic isotope effect determined as $k_{\text{H}}/k_{\text{D}} = 3.0$ at 323 K, which may be ascribed to the proton transfer from $\text{AcrH}_2^{\bullet+}$ to DPPH^- in Scheme 18, is significantly smaller than that in the direct hydrogen-transfer process from AcrH_2 to the nitroxide radical (vide supra). The difference in the mechanism of hydrogen-transfer reactions of nitroxide radicals and DPPH^\bullet may be ascribed to the difference in the one-

electron reduction potentials. The electron-transfer process is much favored in the case of DPPH• which has the positive one-electron reduction potentials (0.24 V) as compared to the negative one-electron reduction potentials of nitroxide radicals (vide supra). The significant steric effect of the bulky substituents of DPPH• may also contribute to favor the electron-transfer pathway, since no significant interaction is required for the electron-transfer process, as compared to an alternative direct hydrogen transfer process which requires the close contact of the reactants.

Not only neutral radicals but also radical anions can abstract hydrogen from BNAH.⁸¹⁾ As is the case of the hydrogen transfer from BNAH to DPPH•, the hydrogen transfer from BNAH to 2,3-dicyano-5,6-dichloro-*p*-benzosemiquinone radical anion (DDQ•[−]) is followed by fast electron transfer from BNA• ($E_{\text{ox}}^0 = -1.1$ V)¹⁶⁾ to DDQ•[−] ($E_{\text{red}}^0 = -0.31$ V)⁸¹⁾ to yield BNA⁺, DDQ^{2−}, and DDQH[−]. The BNAH can also reduce *p*-chloranil radical anion (Cl₄Q•[−]), although the reactivity of Cl₄Q•[−] ($k_{\text{obs}} = 1.1 \times 10^{-1} \text{ dm}^3 \text{ mol}^{-1} \text{ s}^{-1}$) is much smaller than that of DDQ•[−] ($1.1 \times 10 \text{ dm}^3 \text{ mol}^{-1} \text{ s}^{-1}$). To our sur-

prise, the addition of NaClO₄ to the BNAH–Cl₄Q•[−] system results in the increase in the rate of the hydrogen transfer as shown in Fig. 19a, where the k_{obs} value increases linearly with an increase in [NaClO₄].⁸¹⁾ However, no acceleration of the rates is observed in the presence of Bu₄NClO₄ (Fig. 20b).⁸¹⁾ The significant catalytic effect of NaClO₄ on the hydrogen transfer from BNAH to Cl₄Q•[−] is confirmed by the voltammetric study.⁸¹⁾ The reduction peak potential of Cl₄Q•[−] is significantly shifted to the positive direction in the presence of 0.10 mol dm^{−3} NaClO₄ as compared to the position in the presence of 0.10 mol dm^{−3} Bu₄NClO₄. Such a positive shift in the presence of NaClO₄ indicates that the one-electron reduction of Cl₄Q•[−] is accompanied by the complex formation of the one-electron reduced product (Cl₄Q^{2−}) with Na⁺, since no effect of Na⁺ was observed on the electronic spectrum of Cl₄Q•[−]. In fact the redox couple of Cl₄Q/Cl₄Q•[−] is unaffected by the presence of 0.10 mol dm^{−3} NaClO₄ as compared to that in the presence of 0.10 mol dm^{−3} Bu₄NClO₄.⁸¹⁾ On the basis of the catalytic effect of Na⁺ on the one-electron reduction of radical anions, combined with the observation of the large primary kinetic isotope effect ($k_{\text{H}}/k_{\text{D}}=22$), the reaction mechanism of the Na⁺-catalyzed hydrogen transfer from BNAH to Cl₄Q•[−] is given by Scheme 19.⁸¹⁾ The initial electron transfer from BNAH to Cl₄Q•[−] is catalyzed by the presence of Na⁺ due to the complexation with Cl₄Q^{2−}, fol-

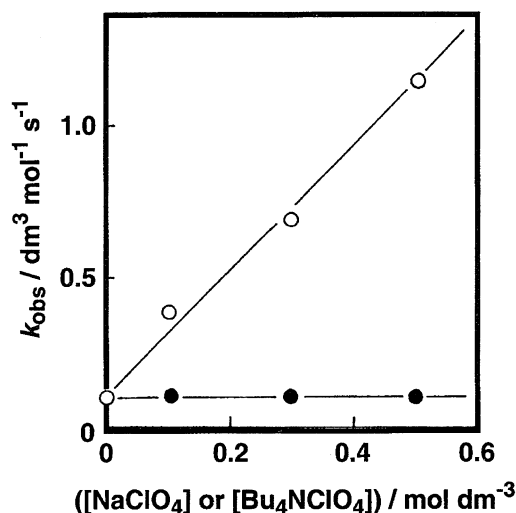
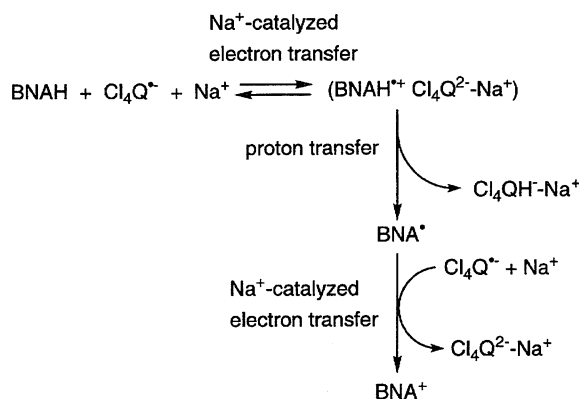


Fig. 20. Plot of k_{obs} vs. [NaClO₄] (○) or [Bu₄NClO₄] (●) for the hydrogen transfer from BNAH to Cl₄Q•[−] ($5.0 \times 10^{-5} \text{ mol dm}^{-3}$) in deaerated acetonitrile at 298 K.



Scheme 19.

Table 3. Fluorescence Maxima (λ_{max}) and the Lifetimes (τ) of Mg²⁺-Carbonyl Complexes, the One-Electron Reduction Potentials (E_{red}^0) of the Singlet Excited States, Fluorescence Quenching Rate Constants (k_q), Rate Constants (k_{et}) of Electron Transfer from RSiMe₃ to the Singlet Excited States, Observed Rate Constants (k_{obs}) and Limiting Quantum Yields (Φ_∞) for Photoaddition of RSiMe₃ to the Carbonyl Compounds in the Presence of Mg(ClO₄)₂ (1.0 mol dm^{−3}) in Acetonitrile at 298 K⁸³⁾

Aromatic carbonyl compound	λ_{max} nm	τ ns	E_{red}^0 vs. SCE ^{a)} V	k_q ^{b)} dm ³ mol ^{−1} s ^{−1}	k_{et} ^{b,c)} dm ³ mol ^{−1} s ^{−1}	k_{obs} ^{b,d)} dm ³ mol ^{−1} s ^{−1}	Φ_∞
2-Naphthaldehyde	440	10.3	1.87	4.3×10^9 (2.3×10^9)	4.5×10^9 (2.2×10^9)	4.6×10^9 (2.3×10^9)	7.1×10^{-2} (1.2×10^{-1})
2'-Acetonaphthone	430	11.8	1.77	3.0×10^9	3.7×10^9	3.5×10^9	1.1×10^{-1}
1-Naphthaldehyde	437	6.7	1.98	4.9×10^9	5.2×10^9	5.4×10^9	9.6×10^{-2}
1'-Acetonaphthone	432	3.3	1.90	3.7×10^9	4.7×10^9	3.9×10^9	1.0×10^{-1}

a) Determined by adaptation of the Rehm–Weller free energy relationship for photoinduced electron transfer. b) Rate constants for PhCH₂SiMe₃. The values in parentheses denote those for CH₂=CHCH₂SiMe₃. c) Calculated by using the Rehm–Weller free energy relationship for photoinduced electron transfer.²²⁾ d) Determined from the quantum yield data.

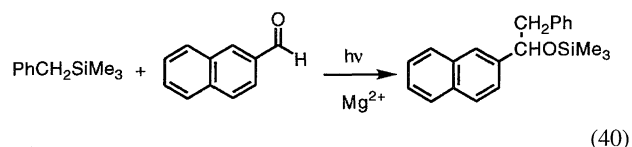
lowed by proton transfer from $\text{BNAH}^{\bullet+}$ to $\text{Cl}_4\text{Q}^{2-}\text{-Na}^+$ to yield BNA^\bullet and Cl_4QH^- . The subsequent electron transfer from BNA^\bullet to $\text{Cl}_4\text{Q}^{\bullet-}$ is fast to yield BNA^+ and Cl_4Q^{2-} (Scheme 19), consistent with the stoichiometry of the overall reaction. According to Scheme 19, the observed rate constant (k_{obs}) may be given by $k_{\text{H}}K_{\text{et}}$, where K_{et} is the equilibrium constant for the endergonic electron transfer and k_{H} is the rate constant of proton transfer from the radical cation to the dianion in the solvent cage. In such a case, the rate constant of overall hydrogen transfer from NADH analogues to radical anions is determined by the energetic of electron transfer and the rate constant of proton transfer. This is essentially the same as the case of hydride transfer from BNAH to *p*-benzoquinone derivatives (Q), in which the rate constant of overall hydride transfer is determined by the energetic of electron transfer from BNAH to Q and the rate constant of proton transfer from $\text{BNAH}^{\bullet+}$ to $\text{Q}^{\bullet-}$, since the second electron transfer from BNA^\bullet to QH^\bullet is highly exergonic. In fact, the k_{obs} value ($7.6 \text{ dm}^3 \text{ mol}^{-1} \text{ s}^{-1}$) of hydride transfer from BNAH to chloro-*p*-benzoquinone which has a similar E_{red}^0 value (-0.34 V) to the E_{red}^0 value of $\text{DDQ}^{\bullet-}$ (-0.31 V) agrees reasonably well with the k_{obs} value (1.1×10) of the hydrogen transfer from BNAH to $\text{DDQ}^{\bullet-}$.⁸¹⁾ Thus, hydrogen transfer from BNAH to the radical anion may occur via stepwise transfer of electron and proton, when the electron transfer is catalyzed even by Na^+ .

Catalysis of Metal Ions on Photoinduced Electron Transfer Reactions. Complexation of metal ions with substrates can not only enhance the oxidizing ability of the substrate, but can also change the excited state property. Aromatic carbonyl compounds with lowest $n\text{-}\pi^*$ singlet states are generally nonfluorescent, possessing large $\pi\text{-}\pi^*$ triplet formation quantum yields (ca. 0.7) via the fast intersystem crossing.⁸²⁾ However, irradiation of the absorption band due to Mg^{2+} complex of 1-naphthaldehyde (1-NA) or 2-naphthaldehyde (2-NA) formed in the presence of $\text{Mg}(\text{ClO}_4)_2$ causes strong fluorescence at 430–440 nm (Table 3).⁸³⁾ The fluorescence lifetimes (τ) of the Mg^{2+} -carbonyl complexes in acetonitrile at 298 K determined by single-photon counting are also listed in Table 3.⁸³⁾ The change in the excited state properties by the complex formation with Mg^{2+} may be attributed to increased energy of the $n\text{-}\pi^*$ singlet state relative to the fluorescent $\pi\text{-}\pi^*$ singlet excited state as reported for similar change in the photophysical and photochemical properties of carbonyl compounds by the complex formation with Lewis acids.⁸⁴⁾ The E_{red}^0 values (vs. SCE) of the singlet excited states of the Mg^{2+} -carbonyl complexes are determined as shown in Table 3 by adaptation of the Rehm–Weller free energy relationship²²⁾ for photoinduced electron transfer from various aromatic electron donors to the singlet excited states of the Mg^{2+} -carbonyl complexes in the presence of Mg^{2+} (1.0 mol dm^{-3}) in acetonitrile at 298 K according to the method reported elsewhere.^{5d,12,19)} The remarkable positive shifts (ca. 1.2 V) of the E_{red}^0 values of the singlet excited states of the Mg^{2+} -carbonyl complexes as compared with those of the triplet excited states of uncomplexed carbonyl compounds (Table 3) result in a significant increase in the re-

activity of the Mg^{2+} complexes vs. noncomplexed carbonyl compounds in the photoinduced electron transfer reactions.

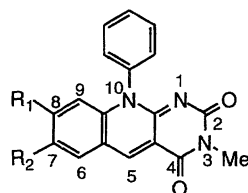
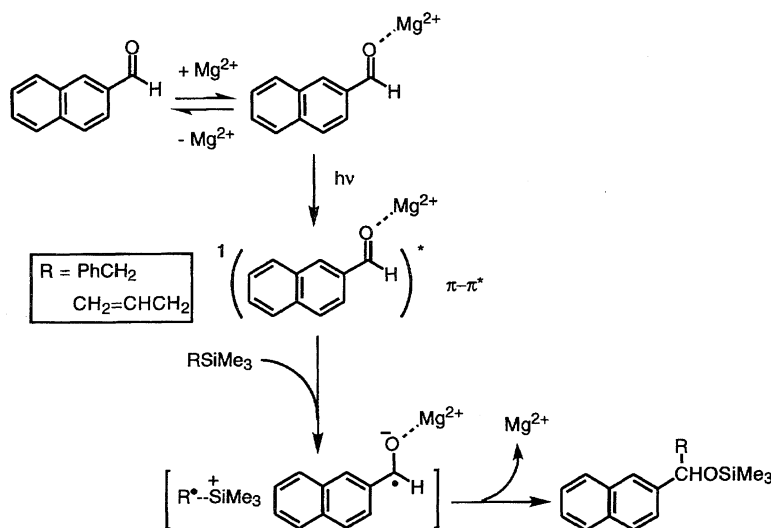
Since the E_{red}^0 values of the singlet excited states of Mg^{2+} -carbonyl complexes become higher than the E_{ox}^0 values of RSiMe_3 ($\text{R}=\text{PhCH}_2, \text{CH}_2=\text{CHCH}_2$) the photoinduced electron transfer from RSiMe_3 to the singlet excited states of Mg^{2+} -carbonyl complexes would occur efficiently. In fact, the fluorescence of Mg^{2+} -carbonyl complexes is quenched efficiently by RSiMe_3 in acetonitrile at 298 K.⁸³⁾ The quenching rate constants k_{q} determined from the slopes of the Stern–Volmer plots and the fluorescence lifetimes are listed in Table 3, where the k_{q} values agree well with the calculated rate constants (k_{et}) of photoinduced electron transfer from RSiMe_3 to the singlet excited states of Mg^{2+} -carbonyl complexes by using the Rehm–Weller free energy relationship.⁸³⁾

Irradiation of the absorption band due to the Mg^{2+} -carbonyl complex in deaerated acetonitrile (0.70 cm^3) containing 2-NA ($5.1 \times 10^{-2} \text{ mol dm}^{-3}$), $\text{PhCH}_2\text{SiMe}_3$ ($1.0 \times 10^{-1} \text{ mol dm}^{-3}$) and $\text{Mg}(\text{ClO}_4)_2$ ($2.0 \times 10^{-1} \text{ mol dm}^{-3}$) with monochromatized light of 360 nm from a xenon lamp in 6.5 h gives the benzyl adduct (70% yield) as shown in Eq. 40.⁸³⁾ The benzyl adducts are also obtained in the photochemical reactions with other carbonyl compounds [1-NA, 1'-acetonaphthone (1-AN), 2'-acetonaphthone (2-AN)] in the presence of Mg^{2+} in acetonitrile.⁸³⁾ When benzyltrimethylsilane is replaced by allyltrimethylsilane ($\text{CH}_2=\text{CHCH}_2\text{SiMe}_3$), the corresponding allyl adducts are also obtained.⁸³⁾



The quantum yields (Φ) of the photoaddition reactions in the presence of $\text{Mg}(\text{ClO}_4)_2$ (1.0 mol dm^{-3}) increase with an increase in $[\text{RSiMe}_3]$ to reach a constant value (Φ_∞). From the standard linear plots of Φ^{-1} vs. $[\text{RSiMe}_3]^{-1}$ are obtained the values of Φ_∞ and the rate constants (k_{obs}), which are also listed in Table 3.⁸³⁾ The k_{obs} values agree well with both k_{q} and k_{et} values. Such agreements strongly indicate that the photoaddition reactions proceed via photoinduced electron transfer from RSiMe_3 to the singlet excited states of Mg^{2+} -carbonyl complexes, followed by the cleavage of R-Si bond in the radical cation and the radical coupling with the carbonyl radical anion to yield the adduct as shown in Scheme 20. Thus, the complexation of Mg^{2+} ion with aromatic carbonyl compounds results in altering the excited states from the triplet states to the singlet states which have the much higher reduction potentials, making it possible to undergo the photoaddition reactions of RSiMe_3 via photoinduced electron transfer.

On the other hand, Mg^{2+} (or Zn^{2+}) ion forms complexes with a flavin analog **1a** (Chart 2) and 5-deazaflavins **2a–c** (Chart 3) with a 1 : 1 stoichiometry in dry acetonitrile at 298 K (Eq. 41),⁸⁵⁾ as the case of NADH analogues (Eq. 33).⁷³⁾ The formation constants K are listed in Table 4. The removal of H_2O from solvent is essential to obtain large formation



2a : $R_1 = \text{H}, R_2 = \text{H}$

2b : $R_1 = \text{Cl}, R_2 = \text{H}$

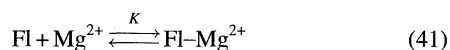
2c : $R_1 = \text{H}, R_2 = \text{NO}_2$

Chart 3.

Table 4. Formation Constants K of the Mg^{2+} and Zn^{2+} Complexes of Flavin **1a** and 5-Deazaflavin Analogs **2a–c** in Acetonitrile at 298 K⁸⁵⁾

	$K/\text{dm}^3 \text{mol}^{-1}$	
	Mg^{2+}	Zn^{2+}
1a	1.7×10^2	4.8×10
2a	1.1×10^3	1.5×10^3
2b	6.4×10^2	9.9×10
2c	1.8×10^2	7.7×10

constants. As such, the addition of small concentrations of H_2O to the Fl-Mg^{2+} system causes a significant decrease in the K value; the K values (1.5×10^2 and $6.5 \times 10 \text{ dm}^3 \text{mol}^{-1}$ in the presence of 2.8×10^{-2} and $8.3 \times 10^{-2} \text{ mol dm}^{-3} \text{H}_2\text{O}$, respectively) become smaller than that ($1.7 \times 10^2 \text{ dm}^3 \text{mol}^{-1}$) in dry acetonitrile where the H_2O concentration is less than $1 \times 10^{-3} \text{ mol dm}^{-3}$.⁸⁵⁾ In fact, no complex formation of **1b** with Mg^{2+} is observed in H_2O .⁸⁵⁾ The metal ion interacts with the C2-carbonyl group of Fl, as is evident from the significant red shift of only the C=O stretching bands due to the C2-carbonyl group of **1a** and **2a–c** in the Mg^{2+} complexes.⁸⁵⁾



Significant enhancement of the oxidizing ability of the singlet excited states of flavin analogues by the complex for-

mation with metal ions is demonstrated in Fig. 21, where the logarithms of the quenching rate constants k_q of $^1\text{Fl}^*$ and $^1\text{Fl}^*-\text{Mg}^{2+}$ (or $^1\text{Fl}^*-\text{Zn}^{2+}$) by various aromatic electron donors are plotted against the oxidation peak potentials of the donors $E_p(\text{D}^{\bullet+}/\text{D})$ as shown by the open and closed or half-closed circles, respectively. The k_q values of the Fl-metal ion complexes are much larger than those of free Fl. The increase of the oxidizing ability of the singlet excited states of Fl by the complex formation with Mg^{2+} or Zn^{2+} is evaluated quantitatively as the positive shifts of $E^0(^1\text{Fl}^*/\text{Fl}^{\bullet-})$, that correspond to the positive shift in the direction of the abscissa $E_p(\text{D}^{\bullet+}/\text{D})$ in Fig. 21. The magnitude of the shift is approximately constant ($0.33 \pm 0.01 \text{ V}$) for different Fl-metal ion complexes.⁸⁵⁾

The complex formation with metal ions not only increases the oxidizing ability of the ground and excited states of Fl but also stabilizes Fl against irradiation of the visible light to prevent the photodegradation. For example, the quantum yield Φ_d of photodegradation of **1a**- Mg^{2+} complex in deaerated acetonitrile is 6.2×10^{-4} which is negligibly small as compared with that of a free flavin **1a** ($\Phi_d = 1.6 \times 10^{-2}$).⁸⁵⁾ Taken together, irradiation of the absorption band of a **1a**- Mg^{2+} complex makes it possible to oxidize *p*-methylbenzyl alcohol to *p*-methylbenzaldehyde, while irradiation of that of a free flavin **1a** results in no dehydrogenation of *p*-methylbenzyl alcohol. Instead, only the predominant photodegradation occurs.^{85,86)}

The reduced flavin- Mg^{2+} complex, $\text{FlH}_2-\text{Mg}^{2+}$ produced in the photooxidation of *p*-methylbenzyl alcohol by Fl-Mg^{2+} is readily oxidized by dioxygen to regenerate the oxidized form Fl-Mg^{2+} .^{85,86)} Thus, flavin-metal ion complexes act as efficient photocatalysts for the dehydrogenation of *p*-methylbenzyl alcohol, as shown in Scheme 21. The photocatalytic dehydrogenation of *p*-methylbenzyl alcohol may be initiated by electron transfer from *p*-methylbenzyl alcohol to the singlet excited state $^1\text{Fl}^*-\text{Mg}^{2+}$, since the rate constant obtained from the Φ dependence on the concentration of *p*-methylbenzyl alcohol agrees well with that obtained independently from the fluorescence quenching of $^1\text{Fl}^*-\text{Mg}^{2+}$.⁸⁵⁾

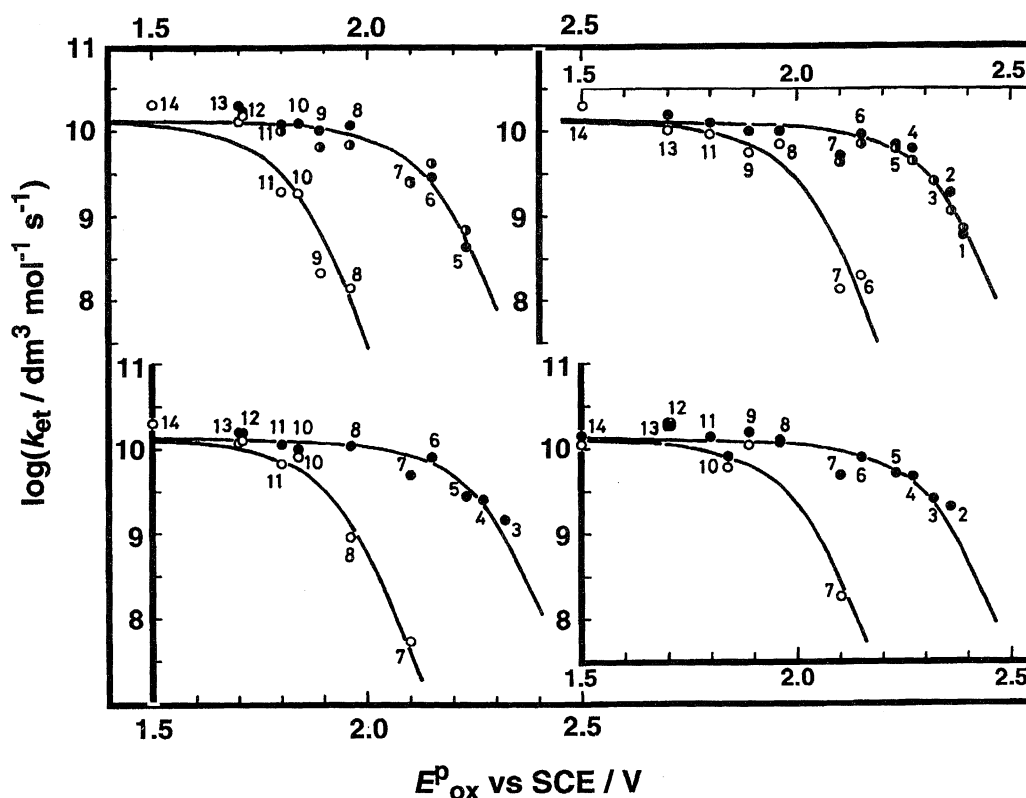
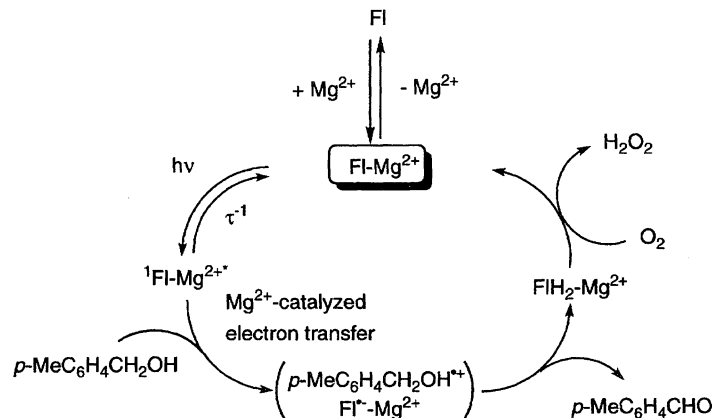
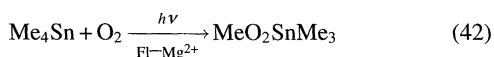


Fig. 21. Plots of $\log k_{\text{et}}$ vs. the oxidation peak potentials of methyl- and methoxy-substituted benzenes (E_{ox}^p) for the fluorescence quenching of flavin analogues (**1a**, **2a**—**c**) by the quenchers in the absence (○) and presence of $0.10 \text{ mol dm}^{-3} \text{ Mg(ClO}_4)_2$ (●) or $\text{Zn(ClO}_4)_2$ (○) in acetonitrile. Numbers refer to the quenchers (e.g., 1=MeC₆H₅, 14=*p*-(MeO)₂C₆H₄).



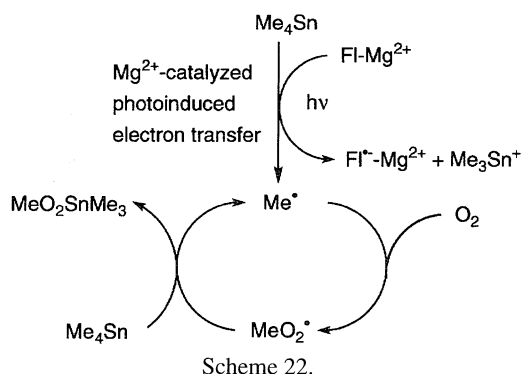
Scheme 21.

Flavin-Mg²⁺ complexes can also catalyze photoinduced oxygenation of R₄Sn via photoinduced electron transfer from R₄Sn to ¹Fl[•]-Mg²⁺ in acetonitrile at 298 K.⁸⁷⁾ For example, irradiation of an oxygen saturated acetonitrile solution containing a flavin analogue **1a**-Mg²⁺ complex and Me₄Sn with visible light results in the formation of MeO₂SnMe₃ (Eq. 42).⁸⁷⁾ Yields of MeO₂SnMe₃ based on the initial amount of **1a** reach 1000% in 15 h, indicating that the **1a**-Mg²⁺ complex acts as a photocatalyst in the photoinduced oxygenation of Me₄Sn.⁸⁷⁾ Neither thermal nor photoinduced oxygenation of Me₄Sn occurs in the absence of the **1a**-Mg²⁺ complex.



The Mg²⁺ ion plays an essential role, since in the absence of Mg²⁺ ion, no photoinduced oxygenation occurs.⁸⁷⁾ The role of Mg²⁺ ion is not only to increase the oxidizing ability of the excited state of **1a** but also stabilize **1a** against irradiation of the visible light to prevent the photodegradation of **1a** by forming the complex (Eq. 41). In fact, the fluorescence of **1a**-Mg²⁺ can be readily quenched by electron transfer from Me₄Sn but no quenching of **1a**^{*} alone occurs.

As shown in Scheme 22, the photoinduced electron transfer from Me₄Sn to Fl[•]-Mg²⁺ initiates the radical chain reactions, similar to those for autooxidation of alkylboranes⁸⁸⁾ and alkylzirconocenes.⁸⁹⁾ No photoinduced electron transfer from Me₄Sn to Fl occurs in the absence of Mg²⁺. Since the one-



electron oxidation of Me_4Sn results in the facile fragmentation of Me_4Sn to yield Me^\bullet ,⁹⁰⁾ the oxygenation of Me_4Sn proceeds by the radical chain reactions. The termination step of primary alkylperoxyl radicals such as MeO_2^\bullet is the bimolecular reaction to give equal amounts of alcohol and aldehyde.⁹¹⁾ The rate-determining step is the $\text{S}_\text{H}2$ reaction of Me_4Sn with MeO_2^\bullet , when the quantum yield increases linearly with an increase in $[\text{Me}_4\text{Sn}]$.⁸⁷⁾

Conclusion

As demonstrated in this review, both thermal and photoinduced electron transfer reactions are accelerated by appropriate third components acting as catalysts when the products of electron transfer form complexes with the catalysts. Such catalysis on electron transfer processes is particularly important to control the redox reactions in which the electron transfer processes are involved as the rate-determining steps followed by facile follow-up steps involving cleavage and formation of chemical bonds. Once the thermodynamic properties of the complexation of acids and metal ions are obtained, we can predict the kinetic formulation on the catalytic activity. We have recently found that various metal ions, in particular rare-earth metal ions, act as very efficient catalysts in electron transfer reactions of carbonyl compounds. The scope and the application of catalysis on electron transfer are expected to expand much further in near future.

The author gratefully acknowledges the contributions of his collaborators mentioned in the references. The author thanks the Ministry of Education, Science, Sports and Culture, for the Grant-in-Aid for Specially Promoted Research.

References

- 1) L. E. Ebersson, "Electron Transfer Reactions in Organic Chemistry; Reactivity and Structure," Springer, Heidelberg (1987), Vol. 25; S. Fukuzumi, in "Advances in Electron Transfer Chemistry," ed by P. S. Mariano, JAI Press, CT (1992), Vol. 2, pp. 67—175.
- 2) S. Fukuzumi and J. K. Kochi, *J. Am. Chem. Soc.*, **102**, 2141 (1980); S. Fukuzumi and J. K. Kochi, *J. Am. Chem. Soc.*, **102**, 7290 (1980); S. Fukuzumi and J. K. Kochi, *J. Am. Chem. Soc.*, **103**, 2783 (1981); S. Fukuzumi and J. K. Kochi, *J. Am. Chem. Soc.*, **103**, 7240 (1981); S. Fukuzumi and J. K. Kochi, *J. Am. Chem. Soc.*, **104**, 7599 (1982); S. Fukuzumi and J. K. Kochi, *Bull. Chem. Soc. Jpn.*, **56**, 969 (1983); R. J. Klingler, S. Fukuzumi and J. K. Kochi, *ACS Symp. Ser.*, **211**, 117 (1983); J. K. Kochi, "Organometallic Mechanisms and Catalysis," Academic Press, New York (1978); J. K. Kochi, *Angew. Chem., Int. Ed. Engl.*, **27**, 1227 (1988); J. K. Kochi, *Acc. Chem. Res.*, **25**, 39 (1992).
- 3) N. Kornblum, *Angew. Chem., Int. Ed. Engl.*, **14**, 734 (1975); J. F. Bunnett, *Acc. Chem. Res.*, **11**, 413 (1978); M. Chanon and M. L. Tobe, *Angew. Chem., Int. Ed. Engl.*, **21**, 1 (1982); M. Chanon, *Acc. Chem. Res.*, **20**, 214 (1987); M. Chanon, M. Rajzmann, and F. Chanon, *Tetrahedron*, **46**, 6193 (1990); J.-M. Savéant, *Acc. Chem. Res.*, **26**, 455 (1993).
- 4) A. Pross, *Acc. Chem. Res.*, **18**, 212 (1985); S. S. Shaik, *Prog. Phys. Org. Chem.*, **15**, 264 (1985).
- 5) M. A. Fox and M. Chanon, "Photoinduced Electron Transfer," Elsevier, Amsterdam (1988), Part A—D; M. Julliard and M. Chanon, *Chem. Rev.*, **83**, 425 (1983); G. J. Kavarnos and N. J. Turro, *Chem. Rev.*, **86**, 401 (1986); F. Müller and J. Mattay, *Chem. Rev.*, **93**, 99 (1993).
- 6) K. Mikami, S. Matsumoto, A. Ishida, S. Takamuku, T. Suenobu, and S. Fukuzumi, *J. Am. Chem. Soc.*, **117**, 11134 (1995).
- 7) K. Maruyama, *Bull. Chem. Soc. Jpn.*, **37**, 897 (1964); K. Maruyama and T. Katagiri, *J. Am. Chem. Soc.*, **108**, 6263 (1986); E. C. Ashby, *Acc. Chem. Res.*, **21**, 414 (1988); M. Newcomb and D. P. Curran, *Acc. Chem. Res.*, **21**, 206 (1988).
- 8) K. Ishikawa, S. Fukuzumi, T. Goto, and T. Tanaka, *J. Am. Chem. Soc.*, **112**, 1577 (1990); K. Ishikawa, S. Fukuzumi, and T. Tanaka, *Inorg. Chem.*, **28**, 1661 (1989).
- 9) R. A. Marcus, *Ann. Rev. Phys. Chem.*, **15**, 155 (1964).
- 10) M. Meites, "Polarographic Techniques," 2nd ed, Wiley, New York (1965), pp. 203—301.
- 11) P. R. Rich and D. S. Bendall, *Biochim. Biophys. Acta*, **592**, 506 (1980); D. Meisel and G. Czapski, *J. Phys. Chem.*, **79**, 1503 (1975).
- 12) S. Fukuzumi, K. Ishikawa, K. Hironaka, and T. Tanaka, *J. Chem. Soc., Perkin Trans. 2*, **1987**, 751.
- 13) S. Fukuzumi, K. Ishikawa, and T. Tanaka, *J. Chem. Soc., Dalton Trans.*, **1985**, 899; K. Ishikawa, S. Fukuzumi, and T. Tanaka, *Inorg. Chem.*, **28**, 1661 (1989).
- 14) NADH and ordinary NADH model compounds are known to be subject to the acid-catalyzed hydration, see: C. C. Johnston, J. L. Gardner, C. H. Suetler, and D.E. Metzler, *Biochemistry*, **2**, 689 (1963); P. van Eikeren, D. L. Grier, and J. Eliason, *J. Am. Chem. Soc.*, **101**, 7406 (1979); E. B. Skibo and T. C. Bruice, *J. Am. Chem. Soc.*, **105**, 3316 (1983).
- 15) S. Fukuzumi, M. Ishikawa, and T. Tanaka, *Chem. Lett.*, **1989**, 1227; S. Fukuzumi, M. Ishikawa, and T. Tanaka, *J. Chem. Soc., Perkin Trans. 2*, **1989**, 1811.
- 16) S. Fukuzumi, S. Koumitsu, K. Hironaka, and T. Tanaka, *J. Am. Chem. Soc.*, **109**, 305 (1987); S. Fukuzumi, N. Nishizawa, and T. Tanaka, *J. Org. Chem.*, **49**, 3571 (1984).
- 17) L. L. Miller and J. R. Valentine, *J. Am. Chem. Soc.*, **110**, 3982 (1988); C. J. Murray and T. Webb, *J. Am. Chem. Soc.*, **113**, 7426 (1991); C. A. Coleman, J. G. Rose, and C. J. Murray, *J. Am. Chem. Soc.*, **114**, 9755 (1992), and references therein.
- 18) M. Ishikawa and S. Fukuzumi, *J. Chem. Soc., Faraday Trans.*, **86**, 3531 (1990).
- 19) D. T. Sawyer and J. L. Roberts, Jr., *Acc. Chem. Res.*, **21**, 469 (1988).
- 20) S. Fukuzumi, M. Chiba, and T. Tanaka, *Chem. Lett.*, **1989**, 31.
- 21) C. R. Boch, J. A. Connor, A. R. Gutierrez, T. J. Mayer, D. G. Whitten, B. P. Sullivan, and J. K. Nagle, *J. Am. Chem. Soc.*, **101**, 969 (1983); R. J. Klingler, S. Fukuzumi and J. K. Kochi, *ACS Symp. Ser.*, **211**, 117 (1983); J. K. Kochi, "Organometallic Mechanisms and Catalysis," Academic Press, New York (1978); J. K. Kochi, *Angew. Chem., Int. Ed. Engl.*, **27**, 1227 (1988); J. K. Kochi, *Acc. Chem. Res.*, **25**, 39 (1992).

4815 (1979).

22) D. Rehm and A. Weller, *Isr. J. Chem.*, **8**, 259 (1970); *Ber. Bunsenges. Phys. Chem.*, **73**, 834 (1969).

23) M. Dixon, E. C. Webb, C. J. R. Thorne, and K. F. Tipton, "Enzymes," 3rd ed, Longman, London (1979).

24) M. Ishikawa and S. Fukuzumi, *J. Chem. Soc., Chem. Commun.*, **1990**, 1353.

25) D. N. Kusanov, Z. N. Parnes, and N. M. Loim, *Synthesis*, **1974**, 633; M. P. Doyle, D. J. DeBruyn, S. J. Donnelly, D. A. Kooistra, A. A. Odubela, C. T. West, and S. M. Zonnebelt, *J. Org. Chem.*, **39**, 2740 (1974).

26) S. Fukuzumi and M. Fujita, *Chem. Lett.*, **1991**, 2059; M. Fujita, S. Fukuzumi, and J. Otera, *J. Mol. Catal.*, **85**, 143 (1993).

27) S. Fukuzumi, Y. Tokuda, T. Kitano, T. Okamoto, and J. Otera, *J. Am. Chem. Soc.*, **115**, 8960 (1993).

28) S. Fukuzumi, S. Mochizuki, and T. Tanaka, *J. Am. Chem. Soc.*, **111**, 1497 (1989).

29) S. Fukuzumi and T. Yorisue, *Chem. Lett.*, **1990**, 871.

30) S. Fukuzumi, S. Kuroda, T. Goto, K. Ishikawa, and T. Tanaka, *J. Chem. Soc., Perkin Trans. 2*, **1989**, 1047.

31) P. F. Heelis, *Chem. Soc. Rev.*, **11**, 15 (1982).

32) S. Fukuzumi, M. Chiba, and T. Tanaka, *J. Chem. Soc., Chem. Commun.*, **1989**, 941; S. Fukuzumi and M. Chiba, *J. Chem. Soc., Perkin Trans. 2*, **1991**, 1393.

33) S. Fukuzumi, M. Ishikawa, and T. Tanaka, *J. Chem. Soc., Perkin Trans. 2*, **1989**, 1037.

34) S. Fukuzumi, T. Kitano, and M. Mochida, *J. Am. Chem. Soc.*, **112**, 3246 (1990).

35) B. P. Mason, "Free Radicals in Biology," ed by W. A. Pryor, Academic Press, New York (1982), Vol. V, p. 161.

36) R. Kaptein, *Chem. Commun.*, **1971**, 732.

37) B. Alberts, D. Bray, J. Lewis, M. Raff, K. Roberts, and J. D. Watson, "Molecular Biology of the Cell," Garland Publishing, New York (1983).

38) Y. Hatefi, *Ann. Rev. Biochem.*, **54**, 1015 (1985); I. E. Hassinen, *Biochim. Biophys. Acta*, **853**, 135 (1986).

39) S. Fukuzumi, S. Mochizuki, and T. Tanaka, *Chem. Lett.*, **1987**, 27; S. Fukuzumi, S. Mochizuki, and T. Tanaka, *Inorg. Chem.*, **28**, 2459 (1989).

40) S. Fukuzumi, S. Mochizuki, and T. Tanaka, *J. Chem. Soc., Chem. Commun.*, **1989**, 391; S. Fukuzumi, S. Mochizuki, and T. Tanaka, *Inorg. Chem.*, **29**, 653 (1990).

41) S. Fukuzumi, T. Goto, K. Ishikawa, and T. Tanaka, *Chem. Lett.*, **1988**, 1923; K. Ishikawa, S. Fukuzumi, T. Goto, and T. Tanaka, *J. Am. Chem. Soc.*, **112**, 1577 (1990).

42) S. Fukuzumi, K. Ishikawa, and T. Tanaka, *Chem. Lett.*, **1986**, 1.

43) S. Fukuzumi and S. Tokuda, *Chem. Lett.*, **1991**, 897; S. Fukuzumi and Y. Tokuda, *J. Phys. Chem.*, **97**, 3737 (1993).

44) S. Fukuzumi and T. Tanaka, "Photoinduced Electron Transfer," ed by M. A. Fox and M. Chanon, Elsevier, Amsterdam (1988), Part C, p. 636, and references therein.

45) S. Fukuzumi, K. Hironaka, and T. Tanaka, *J. Am. Chem. Soc.*, **105**, 4722 (1983); M. Ishikawa and S. Fukuzumi, *J. Am. Chem. Soc.*, **112**, 8864 (1990).

46) S. Fukuzumi, M. Chiba, M. Ishikawa, K. Ishikawa, and T. Tanaka, *J. Chem. Soc., Perkin Trans. 2*, **1989**, 1417.

47) F. G. Bordwell, *Acc. Chem. Res.*, **21**, 456 (1988); M. J. Bausch, C. Guadalupe-Fasano, and A. Koohang, *J. Phys. Chem.*, **95**, 3420 (1991).

48) S. Fukuzumi, S. Mochizuki, and S. Tanaka, *Chem. Lett.*, **1988**, 1983; S. Fukuzumi, S. Mochizuki, and T. Tanaka, *J. Chem.*

Soc., Perkin Trans. 2, **1989**, 1583.

49) T. J. van Bergen, D. M. Hedstrand, W. H. Kruizinga, and R. M. Kellogg, *J. Org. Chem.*, **44**, 4953 (1979); C. Pac, M. Ihama, M. Yasuda, Y. Miyauchi, and H. Sakurai, *J. Am. Chem. Soc.*, **103**, 6495 (1981); K. Hironaka, S. Fukuzumi, and T. Tanaka, *J. Chem. Soc., Perkin Trans. 2*, **1989**, 1705; O. Ishitani, S. Yanagida, S. Takamuku, and C. Pac, *J. Org. Chem.*, **52**, 2790 (1987).

50) S. Fukuzumi, S. Mochizuki, and T. Tanaka, *J. Phys. Chem.*, **94**, 722 (1990).

51) S. Fukuzumi, S. Kuroda, and T. Tanaka, *J. Chem. Soc., Chem. Commun.*, **1986**, 1533; S. Fukuzumi, T. Kitano, and T. Tanaka, *Chem. Lett.*, **1989**, 1231.

52) M. Fujita and S. Fukuzumi, *J. Chem. Soc., Perkin Trans. 2*, **1993**, 1915; S. Fukuzumi, M. Fujita, and J. Otera, *J. Chem. Soc., Chem. Commun.*, **1993**, 1536.

53) M. Fujita and S. Fukuzumi, *J. Chem. Soc., Chem. Commun.*, **1993**, 1528.

54) M. Fujita, A. Ishida, T. Majima, S. Fukuzumi, and S. Takamuku, *Chem. Lett.*, **1995**, 111; M. Fujita, A. Ishida, S. Takamuku, and S. Fukuzumi, *J. Am. Chem. Soc.*, **118**, 8566 (1996).

55) F. G. Bordwell, J.-P. Cheng, M. J. Bausch, and J. E. Bases, *J. Phys. Org. Chem.*, **209**, 1 (1988).

56) E. Baciocchi, F. D'Acunzo, C. Galli, and O. Lanzalunga, *J. Chem. Soc., Perkin Trans. 2*, **1996**, 133; E. Baciocchi, T. D. Giacco, and F. Elisei, *J. Am. Chem. Soc.*, **115**, 12290 (1993).

57) C. J. Schlesener, C. Amatore, and J. K. Kochi, *J. Am. Chem. Soc.*, **106**, 7472 (1984); C. J. Schlesener, C. Amatore, and J. K. Kochi, *J. Phys. Chem.*, **90**, 3747 (1986).

58) K. S. Peters, E. Pang, and J. Rudzki, *J. Am. Chem. Soc.*, **104**, 5535 (1982); A. T. Poulos, G. S. Hammond, and M. E. Burton, *Photochem. Photobiol.*, **34**, 169 (1981).

59) D. D. M. Wayner, D. J. McPhee, and D. Griller, *J. Am. Chem. Soc.*, **110**, 132 (1988); B. A. Sim, P. H. Milne, D. Griller, and D. D. M. Wayner, *J. Am. Chem. Soc.*, **112**, 6635 (1990).

60) S. Fukuzumi and T. Okamoto, *J. Am. Chem. Soc.*, **115**, 11600 (1993).

61) For the absorption spectrum of $Q^{\bullet-}$ in the absence of Mg^{2+} in acetonitrile, see: S. Fukuzumi and T. Yorisue, *J. Am. Chem. Soc.*, **113**, 7764 (1991).

62) S. Fukuzumi, K. Ishikawa, and T. Tanaka, *Chem. Lett.*, **1984**, 421; S. Fukuzumi, K. Ishikawa, and T. Tanaka, *Nippon Kagaku Kaishi*, **1985**, 62.

63) S. Fukuzumi and T. Okamoto, *J. Chem. Soc., Chem. Commun.*, **1994**, 521.

64) S. Fukuzumi, T. Kitano, and K. Mochida, *J. Am. Chem. Soc.*, **112**, 3246 (1990).

65) S. Fukuzumi, T. Kitano, and M. Ishikawa, *J. Am. Chem. Soc.*, **112**, 5631 (1990).

66) S. Fukuzumi and Y. Tokuda, *Chem. Lett.*, **1991**, 1909; S. Fukuzumi and Y. Tokuda, *J. Phys. Chem.*, **96**, 8409 (1992).

67) S. Fukuzumi, Y. Tokuda, Y. Chiba, L. Lucedio, P. Carloni, and E. Damiani, *J. Chem. Soc., Chem. Commun.*, **1993**, 1575.

68) G. Maier, *Angew. Chem., Int. Ed. Engl.*, **27**, 1227 (1988).

69) S. Fukuzumi and J. K. Kochi, *Tetrahedron*, **38**, 1035 (1982).

70) S. Yamago, S. Ejiri, M. Nakamura, and E. Nakamura, *J. Am. Chem. Soc.*, **115**, 5344 (1993); M. Dern, H.-G. Korth, G. Kopp, and R. Sustmann, *Angew. Chem., Int. Ed. Engl.*, **24**, 337 (1985).

71) K. T. Finley, "The Chemistry of the Quinoid Compounds," ed by S. Patai, Wiley-Interscience, New York (1974), Part 2, p. 877; K. Kanematsu, S. Morita, S. Fukushima, and E. Osawa, *J. Am. Chem. Soc.*, **103**, 5211 (1981).

72) D. S. Sigman, J. Hajdu, and D. J. Creighton, "Bioorganic

Chemistry," ed by E. E. van Tamelen, Academic Press, New York (1978), Vol. IV, p. 385, and references therein.

73) S. Fukuzumi, Y. Kondo, and T. Tanaka, *Chem. Lett.*, **1983**, 485.

74) S. Fukuzumi, N. Nishizawa, and T. Tanaka, *J. Chem. Soc., Perkin Trans. 2*, **1985**, 371.

75) T. C. Bruice, *Acc. Chem. Res.*, **13**, 256 (1980); C. Walsh, *Acc. Chem. Res.*, **13**, 148 (1980).

76) G. Eberlin and T. C. Bruice, *J. Am. Chem. Soc.*, **105**, 6685 (1983); E. J. Nanni, Jr., D. T. Sawyer, S. S. Ball, and T. C. Bruice, *J. Am. Chem. Soc.*, **103**, 2797 (1981).

77) Y. Maeda-Yorita and V. Massey, *J. Biol. Chem.*, **268**, 4134 (1993).

78) S. Fukuzumi, S. Kuroda, and T. Tanaka, *J. Am. Chem. Soc.*, **107**, 3020 (1985).

79) Y. Yano, T. Sakaguchi, and M. Nakazato, *J. Chem. Soc., Perkin Trans. 2*, **1984**, 595.

80) E. M. Kosower, "Free Radicals in Biology," ed by W. A. Pryor, Academic Press, New York (1976), Vol. II, Chap. 1.

81) S. Fukuzumi and Y. Tokuda, *Chem. Lett.*, **1992**, 1497.

82) D.W. Boldridge, B. L. Justus, and G. W. Scott, *J. Chem. Phys.*, **80**, 3179 (1984); A. Samanta and R. W. Fessenden, *Chem.*

Phys. Lett., **153**, 406 (1988).

83) S. Fukuzumi, T. Okamoto, and J. Otera, *J. Am. Chem. Soc.*, **116**, 5503 (1994).

84) F. D. Lewis, D. K. Howard, and J. D. Oxman, *J. Am. Chem. Soc.*, **105**, 3344 (1983); F. D. Lewis, S. V. Barancyk, and E. L. Burch, *J. Am. Chem. Soc.*, **114**, 3866 (1992).

85) S. Fukuzumi, S. Kuroda, and T. Tanaka, *Chem. Lett.*, **1984**, 1375; S. Fukuzumi, S. Kuroda, and T. Tanaka, *J. Am. Chem. Soc.*, **107**, 3020 (1985).

86) S. Fukuzumi, S. Kuroda, and T. Tanaka, *Chem. Lett.*, **1984**, 417.

87) S. Fukuzumi, S. Kuroda, and T. Tanaka, *J. Chem. Soc., Perkin Trans. 2*, **1986**, 25.

88) A. G. Davies, K. U. Ingold, B. P. Roberts, and R. Tudor, *J. Chem. Soc. B*, **1971**, 698; S. Korcek, G. B. Watts, and K. U. Ingold, *J. Chem. Soc., Perkin Trans. 2*, **1972**, 242.

89) P. B. Brindley and M. J. Scotton, *J. Chem. Soc., Perkin Trans. 2*, **1981**, 419.

90) S. Fukuzumi, M. Mochida, and J. K. Kochi, *J. Am. Chem. Soc.*, **101**, 5961 (1979); S. Fukuzumi, C. L. Wong, and J. K. Kochi, *J. Am. Chem. Soc.*, **102**, 2928 (1980).

91) J. A. Howard, *Adv. Free Radical Chem.*, **4**, 49 (1972).



Shunichi Fukuzumi was born in Nagoya in 1950. He received his Ph. D degree under supervision of Prof. T. Keii and Y. Ono from Tokyo Institute of Technology in 1978. He did postdoctoral work with Professor Jay K. Kochi at Indiana University from 1978 to 1981. After that, he joined the Department of Applied Chemistry of Osaka University and became a professor in 1994. His research interest is centered on mechanisms and catalysis in electron transfer chemistry of various organic compounds (in particular coenzyme analogs), organometallic compounds, and metal complexes.